

NEW MEXICO DEPARTMENT OF TRANSPORTATION

RESEARCH BUREAU

Innovation in Transportation

Monitoring Long-Term In-Situ Behavior of Installed Fiber Reinforced Polymer:

Report I: State of the Art in Structural Health Monitoring
of Bridges and FRP Systems

Prepared by:
University of New Mexico
Department of Civil Engineering
Albuquerque, New Mexico 87131

Prepared for:
New Mexico Department of Transportation
Research Bureau
7500-B Pan American Freeway NE
Albuquerque, New Mexico 87109

In Cooperation with:
The US Department of Transportation
Federal Highway Administration

**Report
NM08TT-02**

JUNE 2009

1. Report No. NM08TT-02		2. Government Accession No.		3. Recipient's Catalog No.	
4. Title and Subtitle Monitoring Long-Term In-Situ Behavior of Installed Fiber Reinforced Polymer Report I: State of the Art In Structural Health Monitoring of Bridges and FRP Systems				5. Report Date June 2009	
				6. Performing Organization Code	
7. Author(s) M. M. Reda Taha, M. Azarbayejani				8. Performing Organization Report No.	
9. Performing Organization Name and Address University of New Mexico Department of Civil Engineering Albuquerque, NM 87131				10. Work Unit No. (TRAIS)	
				11. Contract or Grant No. CO5102	
12. Sponsoring Agency Name and Address Research Bureau New Mexico Department of Transportation 7500-B Pan American Freeway NE Albuquerque, NM 87109				13. Type of Report and Period Covered	
				14. Sponsoring Agency Code	
15. Supplementary Notes					
16. Abstract The objective of this report is to provide information on state of the art in structural health monitoring (SHM) and its application to bridges. The most recent trends in SHM with regard to fiber reinforced polymer (FRP) composites are discussed. Different approaches for structural monitoring using vibration-based and acoustic monitoring are examined and methods implemented in each approach are discussed and critically visited. Further discussion focuses on the challenge of monitoring significantly large structures and the reasons to consider frequency and wavelet analysis for damage detection. The report also discusses the technologies used for monitoring one bridge in Tucumcari, New Mexico located on Interstate 40 (I-40).					
17. Key Words: Structural health monitoring, Wireless monitoring, AASHTO LRFD, Fiber reinforced polymers.			18. Distribution Statement Available from NMDOT Research Bureau		
19. Security Classif. (of this report) None		20. Security Classif. (of this page) None		21. No. of Pages 23	22. Price

**MONITORING LONG-TERM IN-SITU BEHAVIOR OF INSTALLED
FIBER REINFORCED POLYMER**

**Report I: State of the Art in Structural Health Monitoring
of Bridges and FRP Systems**

by

M. M. Reda Taha
M. Azarbayejani
University of New Mexico
Department of Civil Engineering

Prepared for:

New Mexico Department of Transportation, Research Bureau

A Report on Research Sponsored by:

New Mexico Department of Transportation, Research Bureau

In Cooperation with the

U.S. Department of Transportation, Federal Highway Administration

June 2009

NMDOT, Research Bureau
7500-B Pan American Freeway NE
Albuquerque, NM 87109

PREFACE

The purpose of the research reported herein is to provide state of the art in structural health monitoring (SHM) and its application to bridges. The most recent trends in SHM of fiber reinforced polymer (FRP) composites are discussed as well as different approaches for structural monitoring using vibration-based monitoring and acoustic monitoring. Methods implemented in each approach are discussed and critically visited. Further discussion focuses on the challenge of monitoring significantly large structures and the reasons to abandon frequency analysis as the only method for SHM.

NOTICE

The United States Government and the State of New Mexico do not endorse products or manufacturers. Trade or manufacturers' names appear herein solely because they are considered essential to the object of this report. This information is available in alternative accessible formats. To obtain an alternative format, contact the NMDOT Research Bureau, 7500-B Pan American Freeway NE, Albuquerque, NM 87109 (PO Box 94690, Albuquerque, NM 87199-4690) or by telephone (505) 841-9150.

DISCLAIMER

This report presents the results of research conducted by the author(s) and does not necessarily reflect the views of the New Mexico Department of Transportation. This report does not constitute a standard or specification.

ABSTRACT

The objective of this report is to provide information on state of the art in structural health monitoring (SHM) and its application to bridges. The most recent trends in SHM with regard to fiber reinforced polymer (FRP) composites are discussed. Different approaches for structural monitoring using vibration-based and acoustic monitoring are examined and methods implemented in each approach are discussed and critically visited. Further discussion focuses on the challenge of monitoring significantly large structures and the reasons to abandon frequency analysis as the only method for SHM.

The report describes Fiber Brag Grating (FBG) of fiber optic sensors and reports on their use for FRP delamination. The use of artificial intelligence (AI) techniques and statistical methods for damage pattern recognition are also presented. The discussion focuses on the SHM system installed to monitor one bridge in Tucumcari, New Mexico located on Interstate 40 (I-40).

ACKNOWLEDGMENTS

This work is funded by Federal Highway Administration (FHWA) Contract Number CO5102 to New Mexico Department of Transportation (NMDOT) through the Innovative Bridge Research and Deployment (IBRD) program. The authors greatly acknowledge this support. Technical help during design and installation of the SHM system by System of Systems LLC., National Instruments, Inc. and 3B Builders, Inc. is greatly acknowledged. Field support and excellent cooperation from NMDOT District 4 Engineer “Heather Sandoval” and her field crew is highly appreciated.

TABLE OF CONTENTS

PREFACE	I - i
ABSTRACT	I - ii
ACKNOWLEDGMENTS	I - iii
TABLE OF CONTENTS	I - iv
FIGURES	I - v
OBJECTIVE	I - 1
INTRODUCTION	I - 1
VIBRATION-BASED SHM	I - 3
SHM FOR STRUCTURAL COMPOSITES INCLUDING FRP	I - 12
DAMAGE DIAGNOSIS AND PROGNOSIS	I - 14
CONCLUSION	I - 17
REFERENCES	I - 19

FIGURES

Fig. 1 Acceleration of RC bridge observed in the time domain	I - 4
Fig. 2 Acceleration of RC bridge observed in the frequency domain	I - 5
Fig. 3 Acceleration of RC bridge observed in the wavelet domain	I - 7
Fig. 4 Schematic Representation of Wavelet Multi-Resolution (WMRA) Analysis of a Signal	I - 8
Fig. 5 Example decomposition of acceleration signal using WMRA	I - 9
Fig. 6 Schematic Representation of Wavelet Packet Transformation of a Signal ..	I - 9
Fig. 7 Wavelet Packet Analysis of the Acceleration Signal Shown in Fig. 1	I - 11
Fig. 8 Fuzzy Damage Sets Relating the Change in Damage Features to the Severity of Damage in the Structure (Reda Taha et al. 2006)	I - 16
Fig. 9 Possibility Distribution of the Damage Feature Observed in a Model Bridge (Altunok et al. 2007)	I - 16
Fig. 10 Damage Fuzzy Sets as Observed in the ASCE Benchmark Structure (Azarbayejani et al. 2008)	I - 17

OBJECTIVE

The objective of this report is to provide up-to-date analysis of state of the art in structural health monitoring (SHM) systems of bridges and on monitoring fiber reinforced polymers (FRP) strengthening system. The different aspects of SHM are discussed, followed by an overall review of SHM systems of FRP composites for strengthening reinforced concrete structures.

INTRODUCTION

Many recent reports examine the status of the nation's infrastructure and the subsequent need for investment upgrades to the current system. An article in USA Today (1) stated, "*Billions needed to shore up bridges*". The cost covers not only the shoring up of bridges, but also includes keeping a watchful eye on bridges with degrading performance, thereby helping the Departments of Transportation (DOTs) make efficient decisions on future maintenance, repair or full replacement of the nation's bridge infrastructure.

Structural health monitoring (SHM) is the term used to describe the technical activities necessary to keep an eye on infrastructure. SHM incorporates the necessary work to deploy sensors on the structures and to communicate and analyze data acquired by these sensors to detect damage and provide reliable and efficient strategies for structural maintenance and repair. Deploying efficient SHM systems on bridges can provide early warning about potential damage. Moreover, continuous monitoring of bridges might enable the DOTs to transfer from the current classical schedule-based maintenance to condition-based maintenance where maintenance is tied to structural performance which can result in saving millions of dollars while focusing our resources (2).

A classical classification of SHM systems is to separate between active and passive monitoring. In active monitoring, the structural response due to an active (*a priori* known) force applied to the structure is determined. Active monitoring is typically used with seismic evaluation (2). In such case, the monitoring system tries to solve the inverse problem and determine the structural stiffness matrix. Damage can then be identified by detecting losses in the stiffness matrix elements (3). However, the more dominant class of SHM is the passive monitoring system where monitoring is performed to structural response under random loadings without measuring the applied load (4).

The basic components of SHM include data acquisition, data processing, damage detection, damage pattern recognition and structural prognosis to evaluate the structural life. One important aspect in data processing is the need for efficient signal de-noising technique. While many researchers have described SHM systems in the context of anomaly detection (5, 6), major SHM research was focused on feature extraction and pattern recognition. A hierarchical structure of SHM systems was described by Worden and Duijue-Barton (6). Moreover, Farrar et al. (7) provided an in-depth analysis of the status and needs for damage prognosis as an estimate of a system's remaining useful life. Essential damage prognosis research demonstrated that a critical issue to sensing and data acquisition is the need to capture response on varying length and time scales.

Numerous methods are suggested to monitor structures including monitoring structural deformations and strains. However, significant efforts have been directed to examining vibration-based damage detection methods in bridges. The premise of vibration-based SHM is that dynamic characteristics of a structure are a function of its mechanical properties. Thus changes in these mechanical properties as a result of

localized structural damage will result in observable changes in the dynamic characteristics vibrations of the structure. Research on vibration-based damage identification goes back to the late 1970s in the study of offshore oil and gas platforms, as well as in the aerospace industry. A review of vibration-based SHM techniques for damage detection can be found elsewhere (8, 9).

Acoustic monitoring is an alternative approach from vibration-based damage detection that was introduced to the SHM community (10). Tozser and Elliott (11) showed the possible use of this method to monitor cable stayed bridges and post-tensioning cables in bridges. The concept is that fracture of these cables can be monitored. Assessment of the rate of detecting acoustic events can provide an efficient health monitoring system. Damage detection using acoustic emission has been suggested by many researchers. For instance, Carpinteri et al. (12) showed the use of acoustic emission for structural damage detection and prognosis.

VIBRATION-BASED SHM

Several damage metrics (sometimes also referred to as damage features) have been suggested by many researchers for vibration-based SHM. These metrics included natural frequency (13), mode shapes (14) and curvature of mode shapes (15). These damage metrics can be extracted by performing digital signal processing of acceleration signals received from the bridge structure (16, 17). Time and frequency analysis methods have been the most dominant techniques. In frequency analysis Fast Fourier Transform (FFT) is used to identify the major frequency components of the major mode shapes and observe changes in these components as damage happens in the structure. More information on FFT can be found elsewhere (18). A time representation of an

acceleration signal observed using accelerometers installed on a reinforced concrete bridge is shown in Fig. 1. The high acceleration amplitude at 40 seconds is attributed to a heavy truck passing over the bridge at that time.

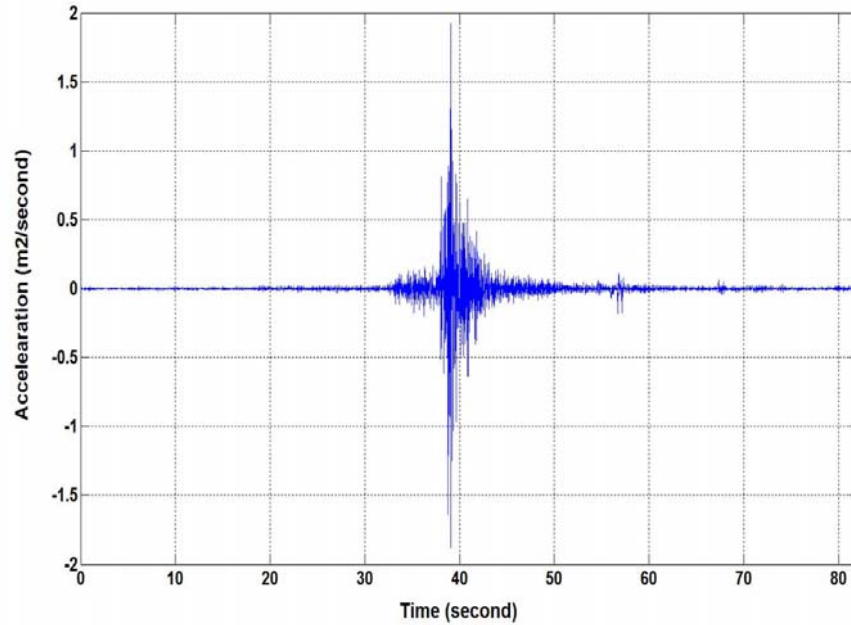


FIGURE 1 Acceleration of RC Bridge in the time domain.

Fig. 2 shows the frequency analysis of the same signal shown in Fig. 1. The figure signal shows the ability of frequency based analysis to identify basic frequency components. However, it is obvious that the frequency analysis completely misses all time information.

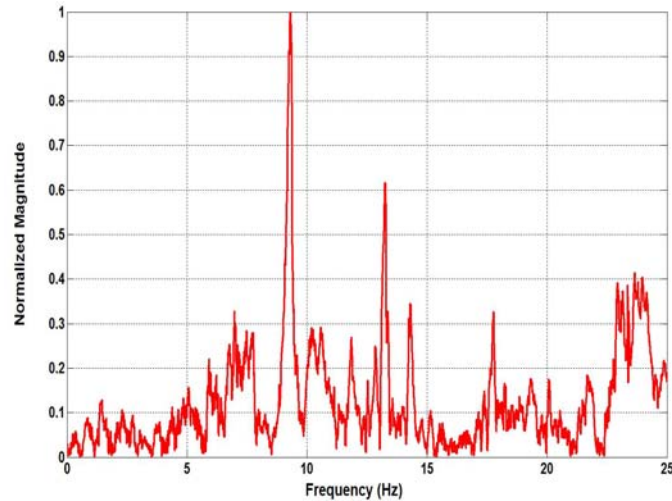


FIGURE 2 Acceleration of RC bridge observed in the frequency domain.

Modal analysis has been also suggested by researchers for identifying damage. Damage detection algorithms from modal analysis depend on observing signals from sensors distributed over the structure and developing accurate structural models (e.g. finite element (FE) models) to identify observable mode shapes. Problems associated with FE modelling such as discretization, configuration errors and modelling errors, as discussed by Yang et al. (19), proved that modal testing might not be sufficiently practical. Moreover, experimental verification of damage detection algorithms using modal data from relatively large structures showed that modal characteristics might be insensitive to localized damage (20). Kim et al. (21) suggested using modal strain energy to estimate the severity of damage and pointed out that changes in the natural frequencies are difficult to measure due to the limited change in frequencies caused by the uneven mass distribution in large structures. Ren and De Roeck (22) examined the effect of noise on the reliability of damage identification from modal analysis and reported that the effect of noise is highly dependent on damage severity such that limited damage states will be more challenging to detect at high levels of noise than severe ones.

Critique was directed to frequency based methods for being heavily dependent on the structural mass (23). While many laboratory experiments showed the ability of frequency metrics to detect damage in small lightweight structures in laboratory settings, field experiments showed very little success in detecting damage in large reinforced concrete bridges using frequency based metrics. The inability to replicate laboratory experiments to field observations for SHM systems is a major challenge in SHM design due to the significant effect of scale on structural response (24).

Such challenge suggested the use of alternative signal analysis methods such as Short Time Fast Fourier Transform (STFT), wavelets (25) and principal component analysis (PCA) (26) for analysis of structural dynamics observations. STFT showed the ability to provide good time and frequency localization as STFT utilizes a window function that is multiplied by the input signal before computing the FFT (27). Although STFT provides a time-frequency representation of a signal, there is a major drawback with respect to utilizing STFT in SHM applications; namely that the width of the window is fixed. Thus, there remains a need for multiple resolution analysis that can provide fine time resolution for long duration signals and fine frequency resolution for high frequency signals (28). A thorough review of various time-frequency techniques for structural vibration analysis is provided by Neild et al. (16). Strengths and weakness of each technique were examined through examining a group of synthetic signals representing possible structural dynamics. Although the review did not address the issue of damage diagnosis it shed light on similarities between these techniques.

On the other hand, wavelet transform (WT) was suggested as an efficient method for digital signal processing that can provide time and frequency information. WT can be

used to obtain vibration signal wavelet coefficients establishing what is known as the wavelet scalogram. Moreover, wavelet multi-resolution analysis (WMRA) can be used to decompose the structural vibration signal into its basic component signals. We discuss both methods here for their major use in structural health monitoring.

The structural acceleration signal presented in Fig. 1 is analyzed here first using WT. Fig. 3 presents a typical scalogram of the wavelet transform of the dynamic response acceleration signal of the bridge.

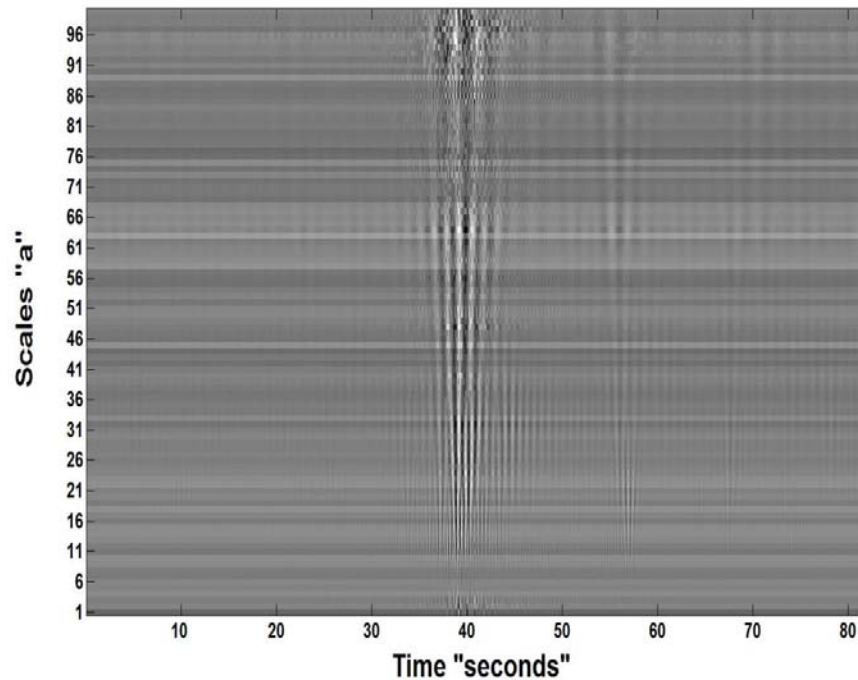


FIGURE 3 Acceleration of RC Bridge observed in the wavelet domain.

The WT is performed using the Morlet mother wavelet showing the variation of the amplitude of wavelet coefficients as variation of the gray color intensities with respect to both time and scale. It is obvious that Fig. 3 is more capable of describing the changes in the system dynamics in both time and frequency domains than Figs. 1 and 2 individually. While a peak acceleration in the structural response is indicated close to 40 seconds, this

peak intensifies at relatively high scale values (relatively stretched wavelets) indicating the existence of high frequency components at this time instant.

Fig. 4 demonstrates a schematic representation of the wavelet multi-resolution decomposition of a signal. An example analysis of the acceleration signal using WMRA is shown in Fig. 5. The dynamic response of the reinforced concrete (RC) bridge that was previously shown in Fig. 1 is decomposed here using the Morlet wavelet at three decomposition levels. Fig. 5 presents the components that constitute this decomposition, including the third level approximation (A3) and the first, second, and third level details (D1, D2 and D3). This process of decomposition can be useful for de-noising or for damage detection in SHM systems. However, this analysis is not limited to one form of WT technology.

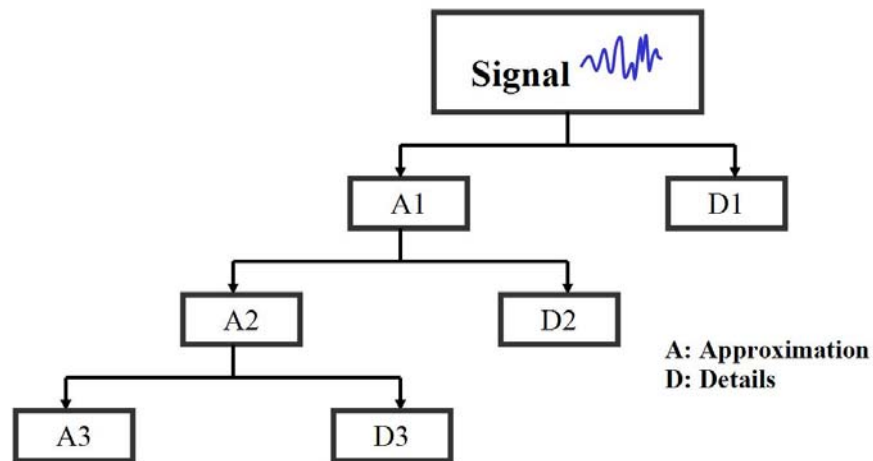


FIGURE 4 Schematic Representation of Wavelet Multi-Resolution Analysis (WMRA) of a Signal.

It is important to note that wavelet analysis of the acceleration signal can make use of the wavelet packet decomposition. Fig. 6 demonstrates a schematic representation of the

wavelet packet decomposition of a signal. Fig. 7 presents the wavelet packet decomposition of the same structural dynamic signal presented in Fig. 1 using the Daubechies wavelet and not the Morlet wavelet with WMRA at three levels of decomposition. The flexibility of wavelet analysis avails itself to the more general use of structural damage detection in the civil infrastructure.

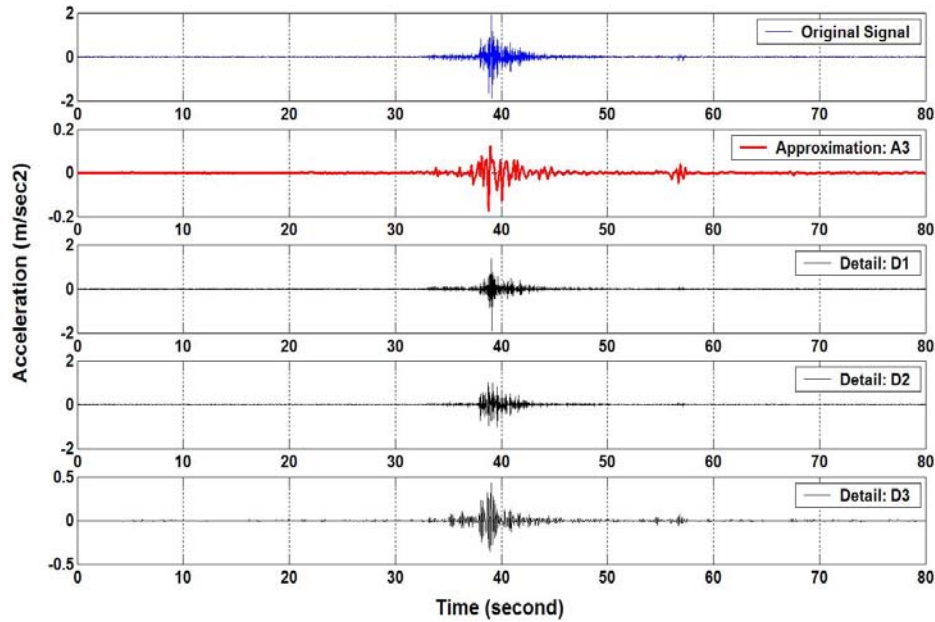


FIGURE 5 Example decomposition of the acceleration signal using WMRA.

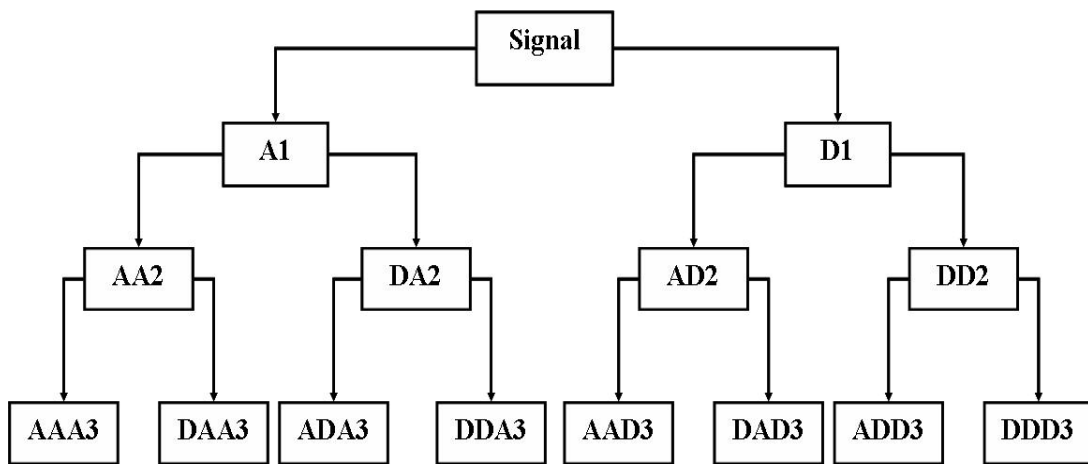


FIGURE 6 Schematic Representation of Wavelet Packet Transformation of a Signal.

As discussed above, wavelets provide an excellent tool for signal processing for damage detection of civil infrastructure. The choice of the wavelet function is an interesting challenge. Many methods have been suggested in the literature to tackle this challenge. Entropy-based criterion has been nominated by a few researchers to be the most successful method for selecting the optimal wavelet function for efficient damage diagnosis (29). Bukkapatnam et al. (5) explained the basic principles of using entropy-based analysis for signal processing. An entropy-based criterion would try to establish a crisp division between systematic signals and noise using means of Shannon's information theory (30). Horton et al. (31) suggested that the most optimal wavelet function is the one that closely resembles the shape features of the acceleration signals.

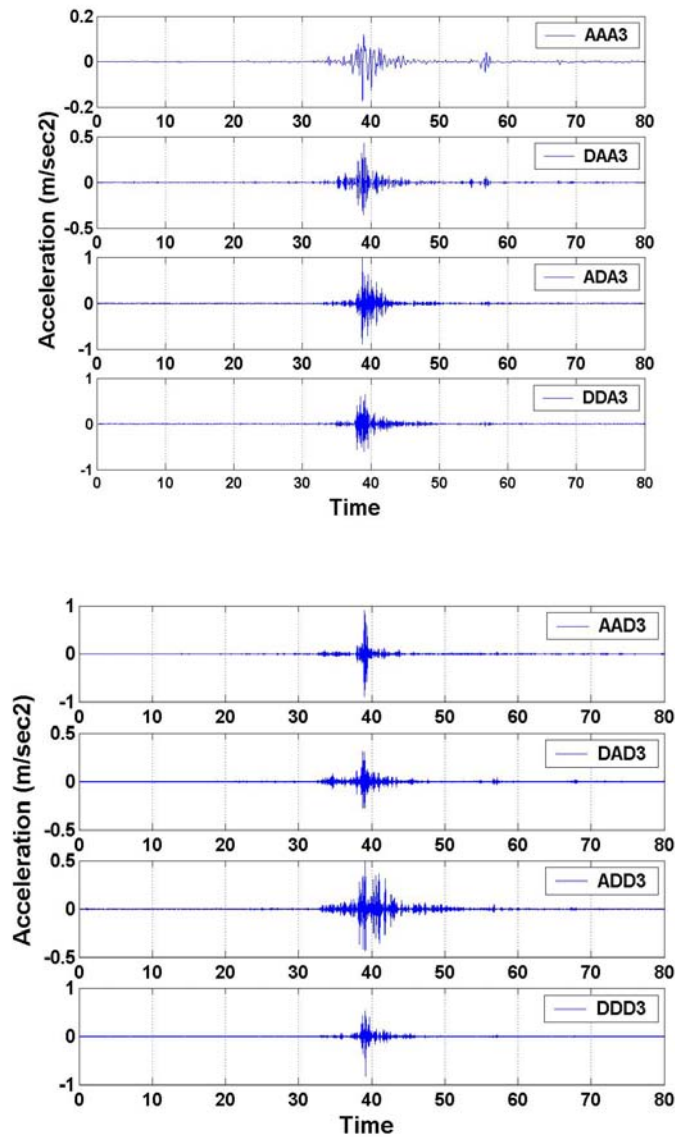


FIGURE 7 Wavelet Packet Analysis of the Acceleration Signal Shown in Fig. 1.

Liew and Wang (32) showed that crack identification of a non-propagating crack in structural systems such as simply supported beams using WT is much more efficient than using PCA. Douka et al. (33) used WT to determine the location and size of the crack in a beam using the fundamental mode of vibration. The size of the crack was related to the wavelet coefficients. Similar work was also reported by Gentile and Messina. (34) who showed that the WT can detect damage location and crack size from both noisy and clean

data. It was argued that damage of machinery parts can be predicted by observing the changes in the wavelet coefficients of the wavelet-transformed vibration signal (35 and 36). Instead of working in the time domain, the spatial wavelet based approach replaces the time variable with a spatial coordinate allowing for the detection and the positioning of a crack.

Experimental and theoretical investigations by Reda Taha et al. (17), Horton et al. (31) and McCuskey et al. (37) showed the possible use of WMRA for damage detection of bridges. It was suggested that the energy of the third approximation signal decomposed using wavelets can be used as the damage feature (17). Other researchers also showed that the energy spectrum in the wavelet packet can be used to detect small structural damage (38). This method is further explained in Report 2 and is used for damage detection in the RC frame bridge in Tucumcari which was recently strengthened with FRP to meet AASHTO 2006 (39) LFRD bridge design specifications.

SHM FOR STRUCTURAL COMPOSITES INCLUDING FRP

On the other hand, damage detection in FRP composite laminates have been suggested by many researchers (40, 41, 42). Strain measurements were considered the most dominant methods for damage detection of FRP. Strain measurement using electrical strain gauges were reported to be useful in detecting fiber debonding (43). However, methods using fiber optical sensors have gained considerable interest in detecting damage in FRP (44 and 45). Significant efforts have been directed for damage detection using Fiber Bragg Grating (FBG) sensors. The concept of FBG is simple, represented by the change of light reflected wavelength when the fibers are strained. Comparison of FBG wavelength of unstrained fibers provides the needed information to calculate the strain by determining

the wavelength shift. Due to its relatively small size, fiber optic sensors have become the most commonly adopted sensing technology for damage detection of FRP composites. New data integration modules can allow recording data from a large number of sensors. FBG sensors can be mounted on the surface of FRP composites used to strengthen RC structures. Using multiplexed FBG provides a profile of strain changes along the FRP plates. FBG sensors have also been reported efficient in field monitoring of FRP (43, 23).

Many researchers have suggested monitoring FRP composites using acoustic sensors. Ultrasonic damage identification methods are common to check damage in composites in the aerospace industry (46). On the other hand, acoustic emission (AE) sensors have been proposed by many researchers (47 and 48). The concept in using AE sensors is based on the realization of the energy released of a material upon fracture. The scale of damage recognized by the AE techniques is dependent on their sensitivity to energy (49). Advances in micro fabrication of micro-electro-mechanical systems (MEMS) enabled the manufacturing of AE sensors that can be embedded in the material (50). A group of new investigations suggested that optical fiber sensors can be sensitive to AE (51). Other efforts examined Rayleigh, shear and lamb waves, with the latter being the most successful (52 and 53). Significant effort is currently performed by researchers worldwide to detect damage location and severity using lamb waves and piezoelectric sensor networks (54). Kessler (49) suggested the use of piezoelectric sensors to identify AE energies in materials. Furthermore, researchers also showed the ability of AE sensors or surface acoustic sensor to identify damage locations by employing large sensor networks (55). A major challenge in using AE surface acoustic and piezoelectric sensors

for damage detection in composite laminates is the need for complex analysis of the received signals to realize damage occurrence.

DAMAGE DIAGNOSIS AND PROGNOSIS

Researchers have shown that using proper domain of each damage metrics can differentiate between healthy and damage cases of bridges (43). The damage state of the structure can be identified by considering effective damage features and by the use of probabilistic methods for classifying these damage features. The use of reference performance to classify the structural health has proven helpful in determining the need for maintenance repair of bridges.

Researchers have combined all the above methods to provide damage diagnosis and prognosis of structures. While damage diagnosis means providing information for damage reasoning, location and severity, damage prognosis is using this former information to predict the service life of the structure (56).

Statistical methods have been attractive tools for damage diagnosis. For instance, Staszewski (57) discussed two approaches for applying statistical pattern recognition in SHM. The first method considered classifying all operating modes of the structures and recognizing any structural response as one of the pre-classified modes. The second method compared any unknown structural response to *a priori*-known healthy response, subsequently, to distinguish the difference between the two responses. While almost all SHM methods utilize one of these two approaches, two major differences between these methods can be recognized. The first is the choice of the feature for building the patterns, and the second is the approach used to aid the damage detection analysis.

Significant research has utilized artificial intelligence (AI) combined with modal analysis to develop the response patterns and to perform efficient feature extraction using artificial neural networks (ANN) (58, 59). Brown et al. (26) demonstrated that cracking introduces a discontinuity to curvatures and deformation time history. Reda Taha and Lucero (60) introduced the use of Bayesian analysis to establish unknown health patterns in bridges. Yan et al. (61) examined the use of statistical methods for extracting the modal parameters of the structure response for detecting structural damage.

Many researchers combined wavelets and neural networks for damage detection and damage pattern recognition. For instance, crack growth in structural concrete was detected using neural networks and was used to provide information about the structural health and the residual service life of the structure. Su and Ye (62) integrated ANN and signal processing to extract what is named as “Digital Damage Fingerprints (DDF)” of the structure. This method was successfully used to detect delamination damage in composite structures.

Other researchers have shown the possible use of fuzzy set theory and possibility theory for damage pattern recognition in structures (63, 64). The use of statistical information to establish fuzzy damage sets for a reinforced concrete structure is shown in Fig. 8. It was found that a fuzzy damage metric can be developed to detect the severity of damage in the reinforced concrete structure.

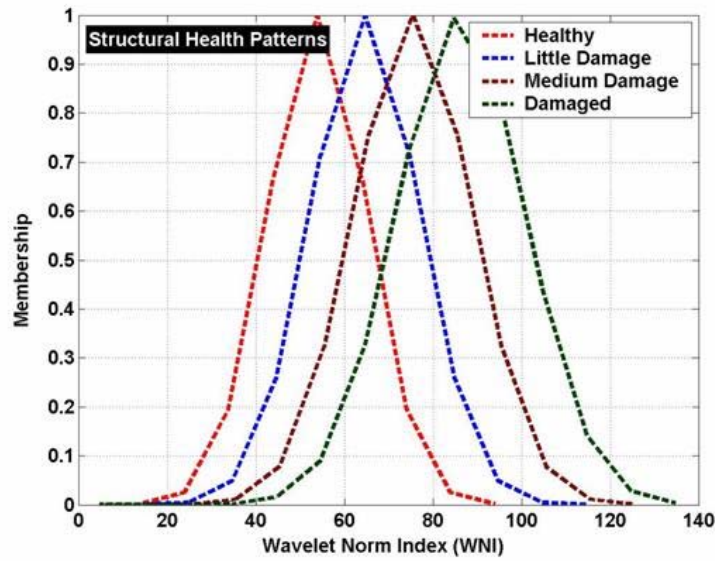


FIGURE 8 Fuzzy Damage Sets Relating the Change in Damage Features to the Severity of Damage in the Structure (63).

Moreover, possibility theory was also shown capable of detecting damage when applied to a model bridge and to a pipeline structure. Possibility distributions for damage detection of a model bridge are shown after Altunok et al. (64) in Fig. 9.

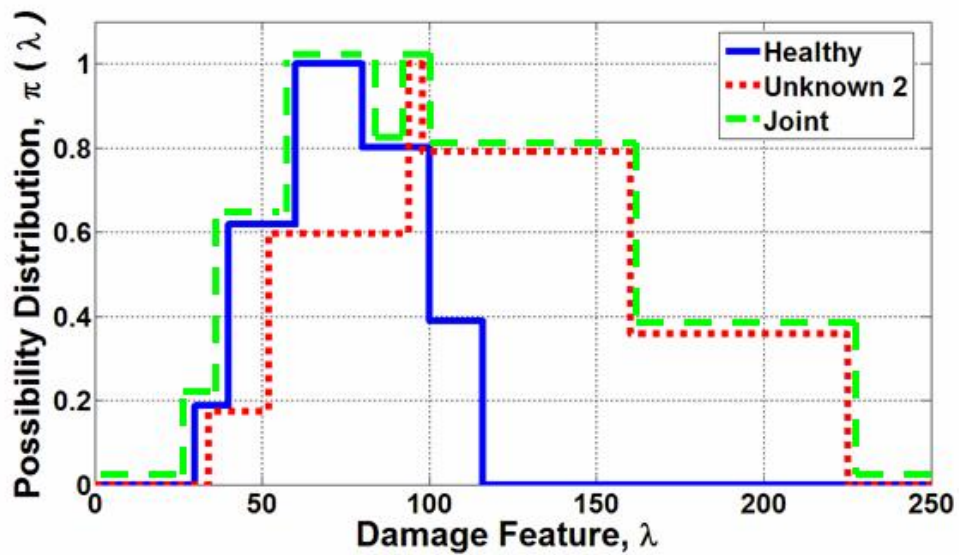


FIGURE 9 Possibility Distribution of the Damage Feature Observed in a Model Bridge (64).

The use of evidence and possibility theory has shown an excellent ability to consider non-statistical uncertainty in damage detection. Consideration of uncertainty allowed for establishing damage sets using principles of minimum entropy (65). A schematic distribution of such damage sets is shown in Fig. 10. The figure also shows how the different severity of damage observations will be located with respect to the damage sets established based on principles of minimum uncertainty.

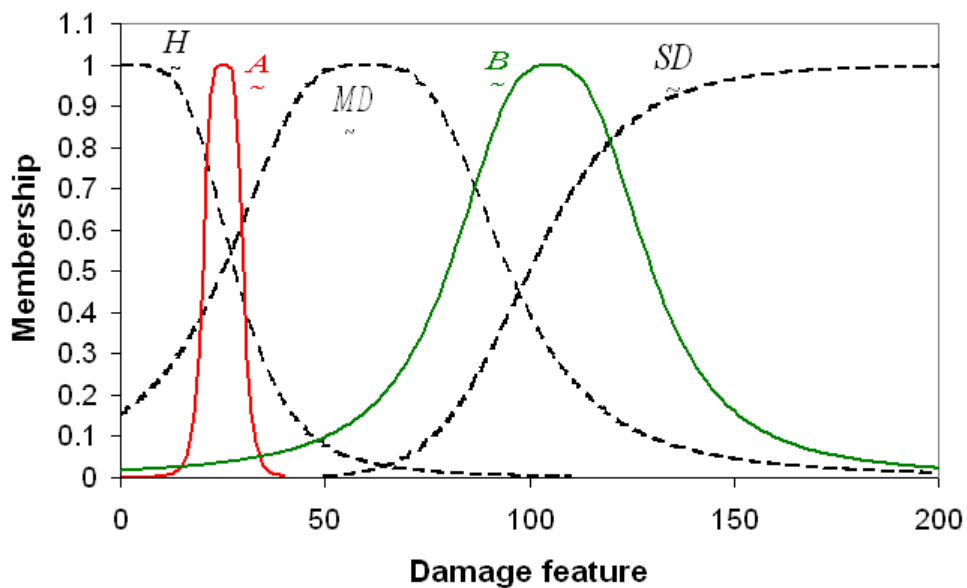


FIGURE 10 Damage Fuzzy Sets as Observed in the ASCE Benchmark Structure (65).

CONCLUSION

This report discusses state of the art in SHM of structures and composite materials. New advances in sensing technology and wireless communication systems have directed SHM systems to remotely monitor infrastructure. By deploying different kinds of sensors including accelerometers, strain gauges and thermocouples, most current SHM systems are capable of measuring the dynamic response of structures. While classical strain

gauges can provide a reasonable set of information for structural composites, most recent research suggests the use of FBG fiber optical sensors or acoustic emission for damage detection of FRP composites. Methods to analyze this data and to establish domains for damage pattern recognition are also discussed at length. The findings in the literature relate to the methods implemented in monitoring the FRP strengthened RC structures in Tucumcari.

REFERENCES

1. USA TODAY. Billions Needed to Shore up Bridges. Friday, July 25, 2008, pp.1 and 10A.
2. Adam, D.E. *Health Monitoring of Structural Materials and Components: Methods and Applications*. John Wiley & Sons, 2007.
3. Zhu, X.Q. and S.S. Law. Damage Detection in Simply Supported Concrete Bridge Structure Under Moving Vehicular Loads. *Journal of Vibration and Acoustics*, Vol. 129, No. 1, 2007, pp. 58-65.
4. Giurgiutiu, V. *Structural Health Monitoring: With Piezoelectric Wafer Active Sensors*. Academic Press, 2007.
5. Bukkapatnam, S.T.S., S.R.T. Kumara and A. Lakhtakia. Analysis of Acoustic Emission Signals in Machining. *ASME Journal of Manufacturing Science and Engineering*, Vol. 121, 1999, pp. 568-576.
6. Worden, K., and J.M. Dulieu-Barton. An Overview of Intelligent Fault Detection in Systems and Structures. *Structural Health Monitoring*, Vol. 3, No. 1, 2004, pp. 85-98.
7. Farrar, C.R., H. Sohn, F.M. Hemez, M.C. Anderson, M.T. Bement, P.J. Cornwell, S.W. Doebling, N. Lieven, A.N. Robertson and J.F. Schultze. *Damage Prognosis: Current Status and Future Needs*. Los Alamos National Lab Report, LA-14051-MS. 2004.
8. Doebling, S.W., C.R. Farrar and M.B. Prime. A Summary Review of Vibration-based Damage Identification Methods. *The Shock and Vibration Digest*, Vol. 30, No. 2, 1998, pp. 91-105.
9. Yong, X. *Condition Assessment of Structures Using Dynamic Data*, Ph.D. Dissertation, School of Civil and Environmental Engineering, Nanyang Technological University, Singapore, 2002.
10. Ohtsu, M. The History and Development of Acoustic Emission in Concrete Engineering. *Magazine of Concrete Research*, Vol. 48, 1996, pp. 321-330.
11. Tozser, O. and J. Elliott. Continuous Acoustic Monitoring of Prestressed Structures. In *3rd Structural Specialty Conference of the Canadian Society of Civil Engineering*, Regina, Saskatchewan, 2000, 6 pp.
12. Carpinteri, A., G. Lacidogna and N. Pugno. Structural Damage Diagnosis and Life-Time Assessment by Acoustic Emission Monitoring. *Engineering Fracture Mechanics*, Vol. 74, 2005, pp. 273-289.
13. Natke, H.G. and C. Cempel. Model-Aided Diagnosis Based on Symptoms, Structural Damage Assessment Using Advanced Signal Processing Procedures. In *Proceedings of DAMAS 97*, UK, 1997, pp. 363-375.

14. Stanbridge, A.B., A.Z. Khan and D.J. Ewins. Fault Identification in Vibrating Structures Using a Scanning Laser Doppler Vibrometer. *Structural Health Monitoring, Current Status and Perspectives*, Stanford University, Palo Alto, California, 1997, pp. 56-65.
15. Ho, Y.K. and D.J. Ewins. On the Structural Damage Identification with Mode Shapes. In *Proceedings of the European COST F3 Conference on System Identification and Structural Health Monitoring*, Madrid, Spain, 2000, pp. 677-686.
16. Neild, S.A., P.D. McFadden and M.S. Williams. A Review of Time-Frequency Methods for Structural Vibration Analysis. *Engineering Structures*, Vol. 25, 2003, pp. 713-728.
17. Reda Taha, M., A. Noureldin, A. Osman and N. El-Sheimy. Introduction to the use of Wavelet Multi-Resolution Analysis for Intelligent Structural Health Monitoring. *Canadian Journal of Civil Engineering*, Vol. 31, No. 5, 2004, pp. 719-731.
18. Humar, J. *Dynamics of Structures*, Second Edition. Balkema Publishers, Rotterdam, The Netherlands. 2002.
19. Yang D.-M., A.F. Stronach and P. MacConnell. The Application of Advanced Signal Processing Techniques to Induction Motor Bearing Condition Diagnosis. *Meccanica*, Vol. 38, No. 2, 2003, pp. 297-308.
20. Friswell, M.I. and J.E.T. Penny. Is Damage Location Using Vibration Measurements Practical? In *Proceedings of the International Workshop: DAMAS 97, Structural Damage Assessment Using Advanced Signal Processing Procedures*, Sheffield, UK, 1997.
21. Kim, J-T., Y-S. Ryu, H-M Choi and N. Stubbs. Damage Identification in Beam-type Structures: Frequency-Based Method vs. Mode-shape-based Method. *Engineering Structures*, Vol. 25, 2003, pp. 57-67.
22. Ren, W-X and G. De Roeck. Structural Damage Identification using Modal Data. I: Simulation Verification. *ASCE Journal of Structural Engineering*, Vol. 128, No. 1, 2002, pp. 87-95.
23. Shrive, P.L., J.P. Newhook, T.G. Brown, N.G. Shrive, G. Tadros and J. Kroman. Thermal Strains in Steel and Glass Fibre Reinforced Polymer Reinforcement in a Bridge Deck. In *Proceedings of the International Conference on Performance of Constriction Materials (ICPCM)*, El-Dieb et al. Eds., Cairo, Egypt, Vol. 1, 2003, pp. 429-437.
24. Shrive, P.L., T.G. Brown and N.G. Shrive. Practicalities of Structural Health Monitoring Systems. *Smart Structures and Systems*, Vol. 5, No. 4, 2009.
25. Hubbard, B. *The World According to Wavelets: The Story of a Mathematical Technique in the Making*. Second Revised Edition. AK Peters, Ltd., Wellesley, Massachusetts, USA. 1998.
26. Browne, M., S. Shiry, M. Don and R. Ouellette. Visual Feature Extraction Via PCA-based Parameterization of Wavelet Density Functions. In *Proceedings of the Third International Symposium on Robots and Automation*, Toluca, Mexico, 2002, pp. 398-402.

27. Robertson, D.C., O. I. Camps, J.S. Mayer and W.B. Gish. Wavelets and Electromagnetic Power System Transients. *IEEE Transaction on Power Delivery*, Vol. 11, No. 2, 1996, pp. 1050-1056.
28. Strang, G. and T. Nguyen. *Wavelet and Filter Banks*. Wellesley-Cambridge Press, NY, USA, 1997.
29. Browne, M., M. Dorn, R. Ouellette, T. Christaller and S. Shiry. Wavelet Entropy-based Feature Extraction for Crack Detection in Sewer Pipes. In *Proceedings of the 6th International Conference on Mechatronics Technology*, Kitakyushu, Japan, 2002, pp. 202-206.
30. Coifman, R.R. and M.V. Wickerhauser. Entropy-based Algorithms for Best Basis Selection. *IEEE Transaction on Information Theory*, Vol. 38, 1992, pp. 713-718.
31. Horton, S., M.M. Reda Taha and T.J. Baca. A Neural-Wavelet Damage Detection Module for Structural Health Monitoring. In *Proceedings of International Workshop on Structural Health Monitoring*, F.-K. Chang, Ed., Stanford, USA, 2005, pp. 556-564.
32. Liew, K.M. and Q. Wang. Application of Wavelet Theory for Crack Identification in Structures. *Journal of Engineering Mechanics*, Vol. 124, No. 2, 1998, pp. 152-157.
33. Douka, E., S. Loutridis and A. Trochidis. Crack Identification in Beams Using Wavelet Analysis. *International Journal of Solids and Structures*, Vol. 40, No. 13-14, 2003, pp. 3557-3569.
34. Gentile, A. and A. Messina. On the Continuous Wavelet Transforms Applied to Discrete Vibrational Data for Detecting Open Cracks in Damaged Beams. *Int. Journal of Solids and Structures*, Vol. 40, No. 2, 2003, pp. 295-315.
35. Moria, K., N. Kasashimaa, T. Yoshiokaa and Y. Uenob. Prediction of Spalling on a Ball Bearing by Applying the Discrete Wavelet Transform to Vibration Signals. *Wear*, Vol. 195, No. 1-2, 1996, pp. 162-168.
36. Masuda, A., A. Nakaoka, A. Sone and S. Yamamoto. Health Monitoring Systems of Structures Based on Orthonormal Wavelet Transform. *Seismic Engineering, Transaction of ASME*, Vol. 312, 1995, pp. 161-167.
37. McCuskey, M., M.M. Reda Taha, S. Horton and T.J. Baca. Identifying Damage in ASCE Benchmark Structure using a Neural-Wavelet Module. In *Proceedings of the International Workshop on Structural Health Monitoring*, Granada, Spain, July 2006, pp. 421-428.
38. Yan, Y.J. and L.H. Yam. Detection of Delamination in Composite Plates Using Energy Spectrum of Structural Dynamic Responses Decomposed by Wavelet Analysis. *Computers and Structures*, Vol. 82, 2004, pp. 347-358.
39. AASHTO. *LRFD Bridge Design Specifications, Manual for Condition Evaluation of Bridges*. American Association of State Highway and Transportation Officials. Interim revisions, Second Edition, Washington, D.C., 2006.

40. Zhao, Y. and F. Ansari. Embedded Fiber Optic Sensor for Characterization of Interface Strains in FRP Composite. *Sensors and Actuators A: Physical*, Vol. 100, No. 2-3, 2002, pp. 247-251.
41. Liang, Y., C. Sun, and F. Ansari. Acoustic Emission Characterization of Damage in Hybrid Fiber Reinforced Polymer Rods. *Journal for Composites for Construction*, Vol. 8, No. 1, 2004, pp. 70-78.
42. Yu, L., L. Cheng, L.H. Yam, Y.J. Yan and J.S. Jiang. Online Damage Detection for Laminated Composite Shells Partially Filled with Fluid. *Composite Structures*, Vol. 80, No. 3, 2007, pp. 334-342.
43. Mehrani, E., A. Ayoub and A. Ayoub. Evaluation of Fiber Optic Sensors for Remote Health Monitoring of Bridge Structures. *Materials and Structures*, Vol. 42, No. 2, 2009, pp. 183-199.
44. Read, I., P. Foote and S. Murray. Optical Fibre Acoustic Emission Sensor for Damage Detection in Carbon Fibre Composite Structures. *Measurement Science and Technology*, Vol. 13, 2002, pp. N5-N9.
45. de Oliveira, R., O. Frazão, J. Ferreira, J.L. Santos and A.T. Marques. In *Proceedings of Third International Conference on NDT*, 15-17 October 2003, Chania - Crete, Greece, 2003.
46. Gros, X.E., K. Ogi and K. Takahashi. Strain and Damage Monitoring of CFRP Laminates by Means of Electrical Resistance Measurement. *Journal of Reinforced Plastics and Composites*, Vol. 17, No. 5, 1998, pp. 389-405.
47. Qi, G., A. Barhorst, J. Hashemi and G. Kamala. Discrete Wavelet Decomposition of Acoustic Emission Signals from Carbon-Fiber-Reinforced Composites. *Composites Science and Technology*, Vol. 57, No. 4, 1997, pp. 389-403.
48. Prosser, W.H. Advanced AE Techniques in Composite Materials Research. *Journal of Acoustic Emission*, Vol. 14, No. 3-4, 1996, pp. S1-S11.
49. Kessler, S.S. *Piezoelectric-Based In-Situ Damage Detection of Composite Materials for Structural Health Monitoring Systems*. PhD Dissertation, Department of Aeronautics and Astronautics, Massachusetts Institute of Technology (MIT), Cambridge, USA. 2002.
50. Schoess, J.N. and J.D. Zook. Test results of Resonant Integrated Microbeam Sensor (RIMS) for Acoustic Emission Monitoring. In *Proceedings of the SPIE Conference on Smart Electronics and MEMS*, Vol. 3328, 1998, pp. 326-332.
51. Lee, J-R. and H. Tsuda. A Novel Fiber Bragg Grating Acoustic Emission Sensor Head for Mechanical Tests. *Scripta Materialia*, Vol. 53, No. 10, 2005, pp. 1181-1186.
52. Wang, L. and F.G. Yuan. Damage Identification in a Composite Plate using Prestack Reverse-time Migration Technique. *Structural Health Monitoring*. Vol. 4, No. 3, 2005, pp. 195-211.
53. Su, Z., L. Ye and X. Bua. A Damage Identification Technique for CF/EP Composite Laminates Using Distributed Piezoelectric Transducers. *Composite Structures*, Vol. 57, No. 1-4, 2002, pp. 465-471.

54. Mamishev, A.V., B.C. Lesieutre and M. Zahn. Optimization of Multi-Wavelength Interdigital Dielectrometry Instrumentation and Algorithms. *IEEE Transaction on Dielectrics and Electrical Insulation*, Vol. 5, 1998, pp. 408-420.
55. Zhou, G. and L.M. Sim. Damage Detection and Assessment in Fibre-Reinforced Composite Structures with Embedded Fibre Optic Sensors – Review. *Smart Materials and Structures*, Vol. 11, 2002, pp. 925-939.
56. Frangopol, D.M., L.C. Neves and A. Petcherdchoo. Health and Safety of Civil Infrastructures: A Unified Approach. In *Proceedings of the 2nd International Workshop on Structural Health Monitoring of Innovative Civil Structures*, A. Mufti and F. Ansari, Eds., Winnipeg, Canada, 2004, pp. 253-264.
57. Staszewski, W.J. Structural and Mechanical Damage Detection Using Wavelets. *The Shock and Vibration Digest*, Vol. 30, No. 6, 1998, pp. 557-472.
58. Barai, S.V. and P.C. Pandey. Vibration Signature Analysis Using Artificial Neural Networks. *ASCE Journal of Computing in Civil Engineering*, Vol. 9, No. 4, 1995, pp. 259-265.
59. Pandey, A.K., M. Biswas and M.M. Samman. Damage Detection From Changes in Curvature Mode Shapes. *Journal of Sound and Vibration*, Vol. 145, No. 2, 1991, pp. 321-332.
60. Reda Taha, M.M. and J. Lucero. Damage Identification for Structural Health Monitoring Using Fuzzy Pattern Recognition. *Engineering Structures*, Vol. 27, No. 12, 2005, pp. 1774-1783.
61. Yan, B., S. Goto and A. Miyamoto. Time-Frequency Analysis Based on Methods for Modal Parameter Identification of Bridge Structure Considering Uncertainty. In *Proceedings of the 2nd International Workshop on Structural Health Monitoring of Innovative Civil Structures*, A. Mufti and F. Ansari, Eds., Winnipeg, Canada, 2004, pp. 453-464.
62. Su, Z. and L. Ye. Lamb. Wave-Based Quantitative Identification of Delamination in CFEP Composite Structures Using Artificial Neural Algorithm. *Composite Structures*, Vol. 66, 2004, pp. 627-637.
63. Reda Taha, M.M., A. Noureldin, J.L. Lucero and T.J. Baca. Wavelet Transform for Structural Health Monitoring: A Compendium of Uses and Features. *Journal of Structural Health Monitoring*, Vol. 5, No.3, 2006, pp. 267-295.
64. Altunok, E., M.M. Reda Taha and T.J. Ross. A Possibilistic Approach for Damage Detection in Structural Health Monitoring. *ASCE Journal of Structural Engineering*, Vol. 133, No. 9, 2007, pp. 1247-1256.
65. Azarbayejani, M., A. El-Osery, K.-K. Choi and M.M. Reda Taha. Probabilistic Approach for Optimal Sensor Allocation in Structural Health Monitoring. *Smart Materials and Structures*, Vol. 17, No. 5, 2008, paper # 055019.



New Mexico Department of Transportation
RESEARCH BUREAU
7500B Pan American Freeway NE
PO Box 94690
Albuquerque, NM 87199-4690
Tel: (505) 841-9145

NEW MEXICO DEPARTMENT OF TRANSPORTATION

RESEARCH BUREAU

Innovation in Transportation

Monitoring Long-Term In-Situ Behavior of Installed Fiber Reinforced Polymer:

Report II: Proposed Monitoring System for
Bridge 7937 in Tucumcari

Prepared by:
University of New Mexico
Department of Civil Engineering
Albuquerque, New Mexico 87131

Prepared for:
New Mexico Department of Transportation
Research Bureau
7500-B Pan American Freeway NE
Albuquerque, New Mexico 87109

In Cooperation with:
The US Department of Transportation
Federal Highway Administration

**Report
NM08TT-02**

JUNE 2009

1. Report No. NM08TT-02		2. Government Accession No.		3. Recipient's Catalog No.	
4. Title and Subtitle Monitoring Long-Term In-Situ Behavior of Installed Fiber Reinforced Polymer Report II: Proposed Monitoring System for Bridge 7937 in Tucumcari				5. Report Date June 2009	
				6. Performing Organization Code	
7. Author(s) M. M. Reda Taha, M. Azarbajani, G. B. Farfan				8. Performing Organization Report No.	
9. Performing Organization Name and Address University of New Mexico Department of Civil Engineering Albuquerque, NM 87131				10. Work Unit No. (TRAIS)	
				11. Contract or Grant No. CO5102	
12. Sponsoring Agency Name and Address Research Bureau New Mexico Department of Transportation 7500-B Pan American Freeway NE Albuquerque, NM 87109				13. Type of Report and Period Covered	
				14. Sponsoring Agency Code	
15. Supplementary Notes					
16. Abstract The purpose of this report is to present the design of an innovative structural health monitoring (SHM) system designed to provide continuous monitoring of Bridge 7937 in Tucumcari, New Mexico. Bridge 7937 was previously strengthened as a showcase strengthening project. The new SHM system is designed as a smart monitoring system based on field programmable gated array (FPGA) technology with minimum human intervention. The system operates wirelessly and is powered with a solar system. The new SHM system allows continuous remote monitoring of the bridge structure for public safety.					
17. Key Words: Structural health monitoring, Wireless monitoring, AASHTO LRFD, Fiber reinforced polymers.			18. Distribution Statement Available from NMDOT Research Bureau		
19. Security Classif. (of this report) None		20. Security Classif. (of this page) None		21. No. of Pages 33	22. Price

**MONITORING LONG-TERM IN-SITU BEHAVIOR OF
INSTALLED FIBER REINFORCED POLYMER**

**Report II: Proposed Monitoring System for
Bridge 7937 in Tucumcari**

by

M. M. Reda Taha
M. Azarbajejani
G. B. Farfan
University of New Mexico
Department of Civil Engineering

Prepared for:
New Mexico Department of Transportation, Research Bureau

A Report on Research Sponsored by:
New Mexico Department of Transportation, Research Bureau

In Cooperation with the
U.S. Department of Transportation, Federal Highway Administration

June 2009

NMDOT, Research Bureau
7500-B Pan American Freeway NE
Albuquerque, NM 87109

PREFACE

The purpose of this report is to present the design of an innovative structural health monitoring (SHM) system designed to provide continuous monitoring of Bridge 7937 in Tucumcari, New Mexico. Bridge 7937 was previously strengthened using carbon fiber reinforced polymer (CFRP) sheets as a showcase strengthening project. The new SHM system is designed as a smart monitoring system based on field programmable gated array (FPGA) technology with minimum human intervention. The system operates wirelessly and is powered with a solar system. The new SHM at Bridge 7937 allows continuous remote monitoring of the bridge structure for public safety.

NOTICE

The United States Government and the State of New Mexico do not endorse products or manufacturers. Trade or manufacturers' names appear herein solely because they are considered essential to the object of this report. This information is available in alternative accessible formats. To obtain an alternative format, contact the NMDOT Research Bureau, 7500-B Pan American Freeway NE, Albuquerque, NM 87109 (PO Box 94690, Albuquerque, NM 87199-4690) or by telephone (505) 841-9150.

DISCLAIMER

This report presents the results of research conducted by the author(s) and does not necessarily reflect the views of the New Mexico Department of Transportation. This report does not constitute a standard or specification.

ABSTRACT

This report presents the design of an innovative structural health monitoring (SHM) system designed to provide continuous monitoring of Bridge 7937 in Tucumcari, New Mexico. Bridge 7937 was previously strengthened using carbon fiber reinforced polymer (CFRP) sheets at one weak point on the bridge as a showcase strengthening project. The proposed SHM system is designed to ensure the effectiveness of CFRP sheets as well as to monitor the structural performance of the bridge.

The proposed monitoring system was calibrated on a model truss bridge built in the Structural Monitoring Laboratory at University of New Mexico (UNM). The new SHM system is vibration-based designed to detect damage in the bridge structure by realizing changes in structural vibration. The new system includes 20 accelerometers, 8 strain gauges and 4 thermocouples. The system is designed as a smart monitoring system based on field programmable gated array (FPGA) technology with minimum human intervention. The system operates wirelessly and is powered with a solar system. The new SHM at Bridge 7937 in Tucumcari, New Mexico allows continuous remote monitoring of the bridge structure for public safety.

ACKNOWLEDGMENTS

This work is funded by Federal Highway Administration (FHWA) Contract Number CO5102 to New Mexico Department of Transportation (NMDOT) through the Innovative Bridge Research and Deployment (IBRD) program. The authors greatly acknowledge this support. Technical help during design and installation of the SHM system by System of Systems LLC., National Instruments, Inc. and 3B Builders, Inc. is greatly acknowledged. Field support and excellent cooperation from NMDOT District 4 Engineer “Heather Sandoval” and her field crew is highly appreciated.

TABLE OF CONTENTS

PREFACE	II - i
ABSTRACT	II - ii
ACKNOWLEDGMENTS	II - iii
TABLE OF CONTENTS	II - iv
TABLES	II - v
FIGURES	II - v
OBJECTIVE	II - 1
BRIDGE DESCRIPTION	II - 1
STRUCTURAL HEALTH MONITORING (SHM)	II - 5
SHM SYSTEM TO MONITOR BRIDGE 7937	II - 7
SMART DATA ACQUISITION (SDA) SYSTEM	II - 11
MODEL BRIDGE FOR TESTING AND CALIBRATING THE SHM SYSTEM	II - 15
DAMAGE DETECTION ON THE MODEL BRIDGE	II - 19
DESIGN OF PHOTOVOLTAIC POWER SYSTEM FOR SMART SHM	II - 24
Electrical Load Estimate	II - 25
Energy Autonomy	II - 25
PVArray Design	II - 26
Charge Controller	II - 29
Time Controller	II - 29
System Layout	II - 30
CONCLUSION	II - 32
REFERENCES.....	II - 33

TABLES

Table 1 Sensor Locations on Bridge 7937.....	II - 9
Table 2 Energy Consumption Estimation for Powering the SHM System at Bridge 7937 in Tucumcari, New Mexico	II - 25
Table 3 Battery System Parameters	II - 26
Table 4 Time Controller Schedule for the PV System for Bridge 7937	II - 30

FIGURES

Fig. 1 Bridge 7937 at Tucumcari	II - 2
Fig. 2 K-Frames of Bridge 7937.....	II - 3
Fig. 3 As Built Structural Drawing of Bridge 7937	II - 4
Fig. 4 FRP Strips Installed on Bridge 7937.....	II - 5
Fig. 5 Schematic Representation of Accelerometer That Will be Used on Bridge 7937	II - 8
Fig. 6 Location of Sensors Used on Bridge 7937	II - 8
Fig. 7 Schematic Locations of Strain Gauges and Thermocouples on FRP Sheets	II - 10
Fig. 8 Schematic Representation of SHM System Shows all its Components as Designed for Bridge 7937	II - 10
Fig. 9 SDA System Showing the Analogue Modules Integrated on the SDA System by National Instrument	II - 12
Fig. 10 SDA System Components and How They Connect With Each Other ...	II - 13
Fig. 11 Block Diagram of the FPGA Module Showing Data Acquisition From Four Analogue Modules (Part I), Interruption Functions for Synchronizing FPGA and Real-Time Modules (Parts II and III) and the Read and Write Process to DMA FIFO (Part IV)	II - 15
Fig. 12 Model Bridge Constructed at UNM Structural Laboratory	II - 16
Fig. 13 CFRP Strip Installed on the Model Bridge Deck with Strain Gauges Installed on the CFRP	II - 17
Fig. 14 Stainless Steel Plant to Mount Accelerometer on the Model and Real Bridge	II - 18
Fig. 15 Real-Time Acceleration Signals Obtained From the SDA System	II - 18

Fig. 16 Acceleration Signals From Four Different Locations on the Model Bridge	II - 19
Fig. 17 Schematic Representation of WMRA Decomposition of the Acceleration Signal	II - 20
Fig. 18 Original Acceleration Signal (Blue) Along with its Approximation 3 Signal (Red) Showing the Ability of Wavelet Decomposition to Smoothen the Observed Signal	II - 21
Fig. 19 Probability of Damage Feature used to Realize Cases of Healthy and Damage Performances at Two Different Sensors Installed on the Prototype Bridge	II - 23
Fig. 20 Web Tools Developed for (a) Data Transfer from the Bridge and (b) Data Rate and Sensor Selection Control on the SDA	II - 24
Fig. 21 Snap Shot of the Webpage Developed for Efficient Data Transfer Using the Worldwide Web	II - 24
Fig. 22 PV System Location (Tucumcari Latitude: 35° 10' 18" N - Longitude: 103° 43' 27" W) and the Proposed Location of Solar Panels to Enable SHM Power	II - 27
Fig. 23 PV System Sun Tracking Schematic	II - 28
Fig. 24 PV Layout of Proposed PV System for 1 Day of Autonomy	II - 31
Fig. 25 Structural System to Support Solar Panels and Attach Them to the Bridge	II - 32

OBJECTIVE

The purpose of this report is to report on the design of an innovative structural health monitoring (SHM) system designed to provide continuous monitoring of Bridge 7937 in Tucumcari, New Mexico. Bridge 7937 was previously strengthened using carbon fiber reinforced polymer (CFRP) sheets at one weak point on the bridge as a showcase strengthening project. The proposed SHM system is designed to ensure the effectiveness of CFRP sheets as well as report on the overall structural performance of the bridge. The proposed monitoring system's calibration and effectiveness in detecting damage is examined on a model truss bridge built in the Structural Engineering Laboratory at University of New Mexico (UNM). The following sections describe all the details of the proposed monitoring system and the calibration process.

BRIDGE DESCRIPTION

Bridge 7937 on Interstate 40 (I-40) in the city of Tucumcari, New Mexico was selected for implementation of the monitoring system. As shown in Figs. 1 and 2, the bridge consists of five reinforced concrete K-Frame girders. The K-Frames form three spans; 42 ft, 104 ft and 42 ft. Each K-frame has a rectangular reinforced concrete cross-section whose depth varies along the length of the bridge. Asphalt overlay is used on the top of Bridge 7937. Moreover, the longitudinal and transverse reinforcements vary along the length of the bridge. Fig. 3 illustrates the cross section and the longitudinal and transverse reinforcements of this bridge.

During the last two decades since the bridge was constructed, the size and weight of trucks passing over I-40 have increased dramatically. Based on AASHTO 2006 (1), it is expected that the moment and shear demand of the current traffic load might exceed

bridge capacity. Previous research by the UNM team showed that the bridge does not have sufficient capacity in negative moment region according to (1). To ensure that Bridge 7937 falls within the state limit requirements of AASHTO code, UNM researchers installed four fiber reinforced polymer (FRP) strips on the bridge in summer 2007. Fig. 4 shows FRP strips installed on Bridge 7937 by the UNM team.



FIGURE 1 Bridge 7937 at Tucumcari.



FIGURE 2 K-Frames of Bridge 7937.

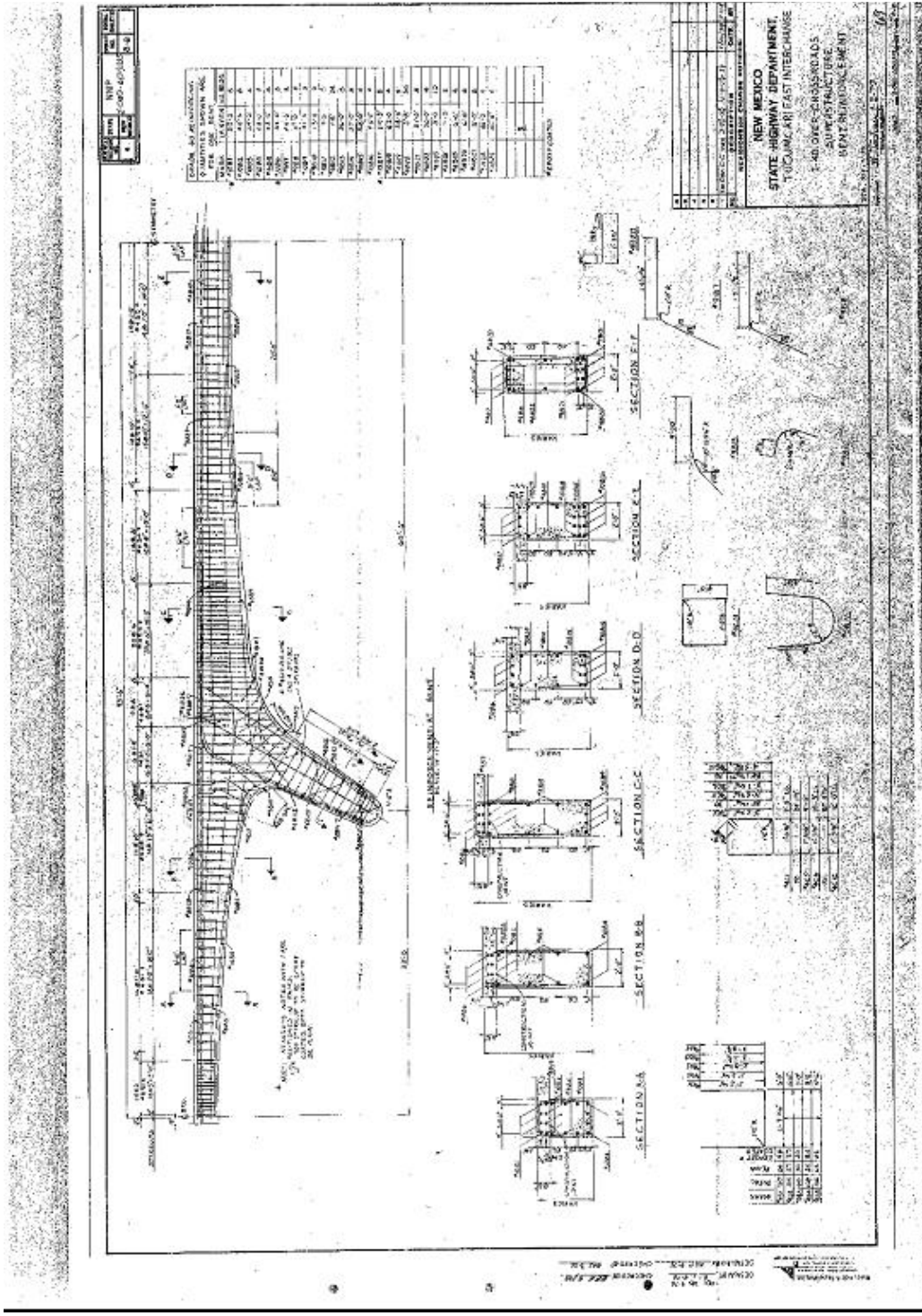


FIGURE 3 As Built Structural Drawing of Bridge 7937.



FIGURE 4 FRP Strips Installed on Bridge 7937.

STRUCTURAL HEALTH MONITORING (SHM)

In the last two decades, SHM systems have developed to accurately and continuously monitor structural response based on real-time loading conditions, detect damage in structures and determine the location and severity of damage. SHM targets the characterization of structural performance to enhance structural safety and reduce lifetime operating costs by early detection for maintenance. Possible detection of damage at its onset, before it has had a chance to propagate, is the major advantage of SHM since it can reduce the potential for catastrophic failure. New innovative methods in SHM systems can inform the department of transportation about potential flaws emerging on bridges without the need for timely visual inspections. Identifying potential flaws on bridges enhances structural safety and reduces operating costs by early damage detection for maintenance. We report here on a vibration-based SHM system that targets damage identification based on monitoring the dynamic response of the structure. The system described here includes monitoring and recording the history of the dynamic response of

the structure during healthy time of performance and observing deviations of that healthy performance.

Using new advances in sensing technology and wireless communication systems have directed SHM systems to remotely monitor infrastructure. By deploying different kinds of sensors including accelerometers, strain gauges and thermocouples, most current SHM systems measure the dynamic response of structures. Conceptually, changes in the dynamic characteristics of a structure (e.g. main frequency components) occur as a result of stiffness reduction of the structure as a result of damage (2, 3). This issue is discussed in detail in Report 1 of this project as part of the state-of-the-art review. Previous investigations showed that structural stiffness reductions may not lead to major changes in frequency components but could lead to changes in the energy of decomposed acceleration signals recorded at a fixed time window (4, 5). The SHM system for monitoring the reinforced concrete (RC) frames at Tucumcari was therefore designed to monitor changes in the energy of acceleration signals as well as changes in the frequency components of a group of sensor networks.

Researchers previously showed that by using proper domain for each damage metric, they could differentiate between healthy and damage cases of bridges (6). The damage state of the structure could be identified by considering effective damage features and the use of probabilistic methods for classifying these damage features. The use of reference performance to classify the structural health proved helpful in determining the need for maintenance repair of bridges.

SHM SYSTEM TO MONITOR BRIDGE 7937

A SHM system consists of a number of sensors that observe structural response, such as accelerations or strains, to acquire and integrate the observations using a data acquisition system. The data collected from data acquisition can then be processed to extract proper monitoring features and patterns that identify structural performance. These patterns can be used at a later time to detect damage occurrence in structures.

The SHM system to monitor Bridge 7937 includes accelerometers and strain gauges along with thermocouples. Twenty accelerometers were used to extract structural dynamic information at different locations on the bridge. The acceleration data was used to extract damage feature(s) which can differentiate between healthy and damage conditions and enable warnings when the bridge is damaged.

To find acceleration on different locations of the bridge, model 333B50 accelerometer from PCB, Inc. was utilized. This model is a piezoelectric accelerometer that has a frequency range of 0.5 to 3 kHz and operates with 1000 mV/g sensitivity, which means an accelerometer produces 1000 mille volt (1 volt) for the acceleration of gravity ($g = 9.8 \text{ m/ sec}^2$ or 32.2 ft/sec^2). Moreover, these accelerometers are stud mounted, which makes them stable on the bridge. Fig. 5 illustrates a schematic for the accelerometer used in monitoring accelerations of Bridge 7937.

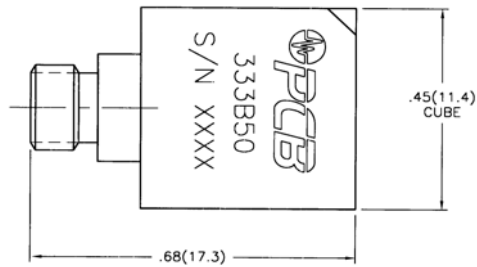
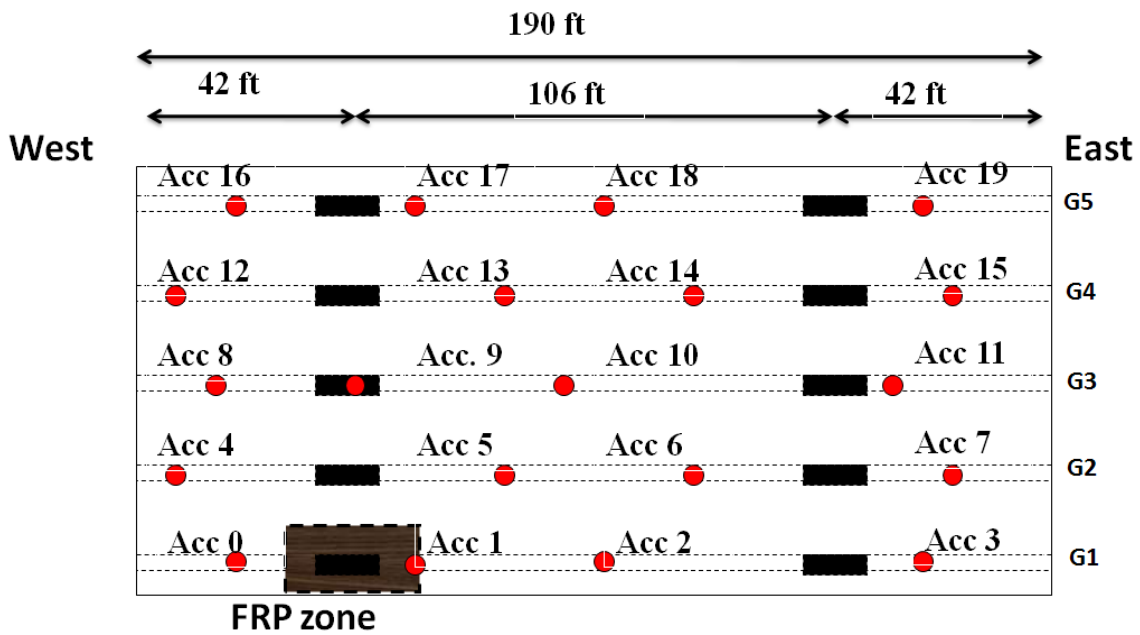


FIGURE 5 Schematic Representation of Accelerometer That Will be Used on Bridge 7937.

Accelerometers were mounted at the bottom slab of the bridge, close to each girder. Accelerometers are shown with their placement location in Fig. 6. As shown in the figure, four accelerometers are installed on each girder of the bridge. Accelerometer placement is determined based on locations of maximum vibration and those locations more prone to cracking. Exact accelerometer locations are provided in Table 1.



-For exact accelerometer locations see Table

- 8 Strain gauges to model debonding are located in FRP zone

FIGURE 6 Location of Sensors Used on Bridge 7937.

TABLE 1 Sensor Locations on Bridge 7937

Girder	Sensor	Location	Sensor	Location	Sensor	Location	Sensor	Location
G1	Acc 0	30	Acc 1	48	Acc 2	100	Acc 3	175
G2	Acc 4	20	Acc 5	80	Acc 6	140	Acc 7	180
G3	Acc 8	25	Acc 9	35	Acc 10	95	Acc 11	165
G4	Acc 12	20	Acc 13	80	Acc 14	140	Acc 15	180
G5	Acc 16	30	Acc 17	48	Acc 18	100	Acc 19	175

- All locations are measured on each girder from west side

To monitor the effectiveness of FRP sheets, strain gauges are also distributed over the FRP application zone. By comparing the strain data of FRP sheets to strains on the concrete surface, the maximum strain due to the traffic and environmental loadings on FRP sheets can be monitored, While it is anticipated that traffic loading will produce very little strain in FRP sheets (in the range of 20-30 microstrains), as observed under load test, it is believed that the very low measurements will change if FRP debonding takes place on the bridge surface. Therefore, the FRP strains are basically used to detect possible FRP debonding.

Moreover, thermocouples are placed on the top and bottom surfaces of the bridge at several locations in order to find the temperature gradient on the bridge and thus monitor strain changes due to temperature change. It is well known that most of the cracks on the bridge are induced because of temperature gradient effects and thus correlating changes in behavior to thermal effects is of great interest. Fig. 7 shows the schematic locations of strain gauges and thermocouples on FRP sheets.

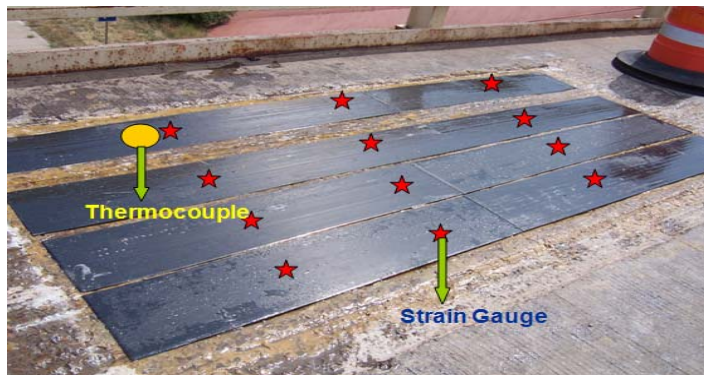


FIGURE 7 Locations of Strain Gauges and Thermocouples on FRP Sheets.

All sensors are connected by wires to a smart data acquisition (SDA) system as described in the next section of this report. The SDA system has the ability to connect the data to NMDOT using a wireless system. The data can then be downloaded to NMDOT using HTTP or FTP internet protocols. A schematic representation of the SHM system and all of its components used in Bridge 7937 is represented in Fig. 8.

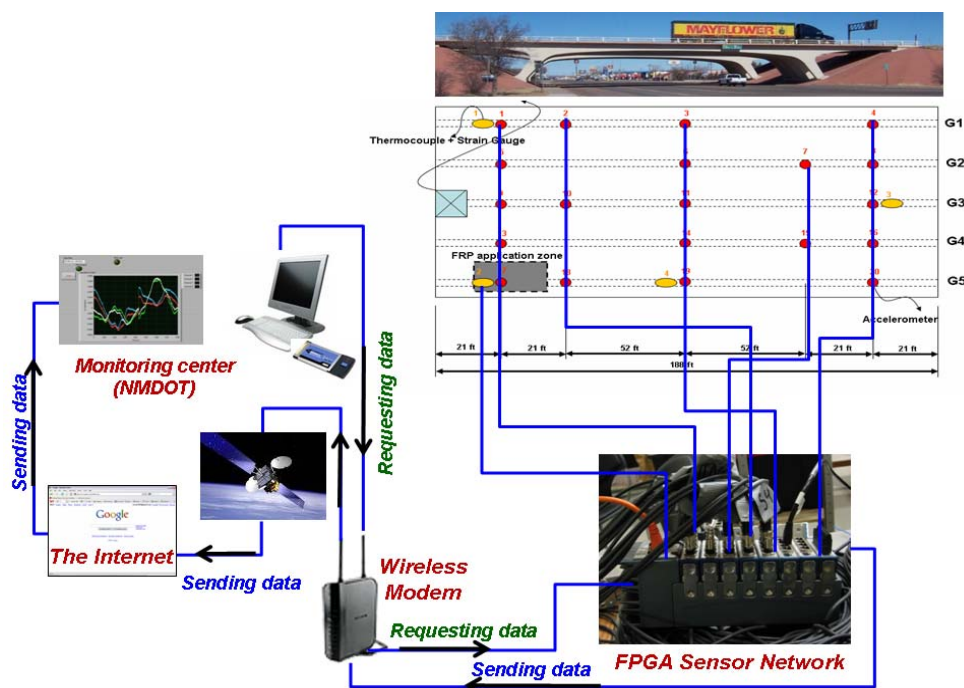


FIGURE 8 Schematic Representation of SHM System Shows all its Components as Designed for Bridge 7937.

SMART DATA ACQUISITION (SDA) SYSTEM

A new data acquisition system for acquiring data from all the sensors is developed to be used on Bridge 7937. The new data acquisition system utilizes a data acquisition platform that consists of two different parts: 1) a real-time controller that has volatile memory and nonvolatile memory for data storage. The real-time controller also encompasses an Ethernet port with built-in file servers allowing access by HTTP and FTP, and 2) a multi-slot reconfigurable chassis that contains Field Programmable Gate Arrays (FPGA) and a Peripheral Component Interface (PCI) bus interface that connects between the FPGA and the real-time controller. This built-in data transfer protocol is used to communicate data to the controller where post processing, data logging and communication to a host computer can take place. The FPGA chip connects directly to the analogue input modules using FPGA functions. Different types of sensors can be connected to different types of analogue modules. We denote the system here as Smart Data Acquisition (SDA) system for its ability to incorporate programmable logic on the hardware. Fig. 9 shows this SDA system, including the controller and eight slot chassis where different modules connect to the chassis. The SDA system has a commercial brand name (Compact Rio[®]) produced by National Instruments (NI).



FIGURE 9 SDA System Showing the Analogue Modules Integrated on the SDA System by National Instrument.

The SDA system replaces the conventional data loggers and computer modules that have been long used for SHM systems. This is achieved by integrating both data acquisition and computational logic gates on the same hardware. The SDA system also has the ability to connect to the worldwide web using wireless modems. Field implementation of the SDA system will enable establishing smart wireless SHM where damage feature extraction protocols can be processed at the bridge site. Therefore, the SDA system enables a unique opportunity for establishing SHM where data transfer can be limited to take place only when needed. Limitation of data transfer not only helps reduce the cost of the SHM system, but it also prevents data overflow reported by many researchers where the SHM system becomes a burden rather than an aide for engineers (7). Moreover, the use of FPGA technology and real-time controllers enables synchronizing signals received from different sensors in real-time as well as the ability for remote hardware reconfigurability. This overcomes a fundamental challenge met by many conventional data loggers.

Developing data acquisition applications to operate on the SDA requires building a system that consists of three different modules, each operating at a different level. Fig. 10 shows schematic representation of three modules and how they connect with each other.

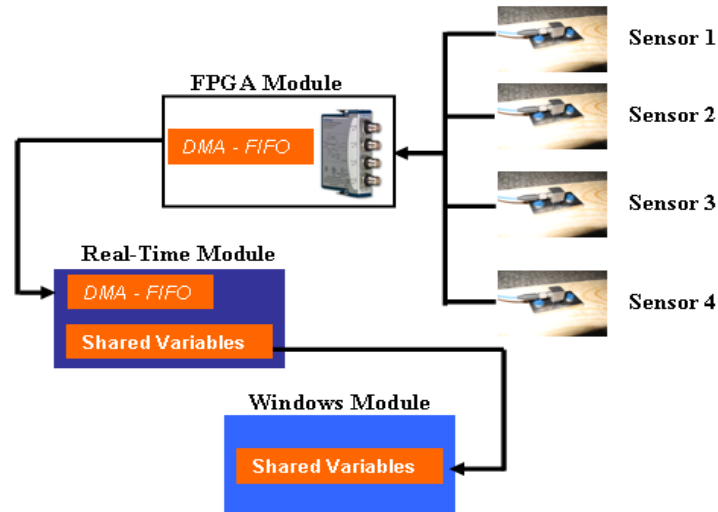


FIGURE 10 SDA System Components and How They Connect With Each Other.

These modules include:

1. FPGA module This module is a low level program coded on FPGA. FPGA is a semiconductor device that can be reconfigured. An FPGA consists of logic blocks, I/O blocks and interconnection wires and switches. Interconnection wires are organized in horizontal and vertical routing channels running between the logic blocks.
2. Real-time module This module is a program coded on the controller of SDA. The controller receives the data from the FPGA module and keeps it in the nonvolatile memory of the SDA system. Using FPGA read/write control function through the PCI bus, the real-time module gets connected with the FPGA module. To transfer data from the FPGA module directly to the SDA real-time controller, Direct Memory Access First

In First Out (DMA FIFO) buffers are used where the first data item written to memory is the first item read and removed from memory.

3. Windows™ host module This module runs on the host computer. This is Windows™ based software, coded in any language, where simple graphical user interface and user friendly options can be developed. The Windows™ module communicates with the SDA system through wireless link and the data is transmitted via the worldwide web. Shared variables are used to communicate between real-time and Windows™ modules.

To make a complete embedded (self-contained) SHM system that communicates the data wirelessly, the FPGA module communicates the data to the real-time module via the DMA FIFO. The data is then saved on the SDA nonvolatile memory in the real-time module. In the next step, the data is transferred through a FTP to the host computer where the Windows™ module operates at the host computer. Fig. 11 illustrates a block diagram describing the program implemented at the FPGA module for the prototype bridge monitoring. Part I of the FPGA module enables converting the binary data acquisition from four analogue data modules to engineering unit data. Parts II and III show how the data rate is identified, the interrupt function to synchronize the FPGA, and the real-time modules as explained above. Part IV in the block diagram also shows how the binary data is written on the DMA FIFO.

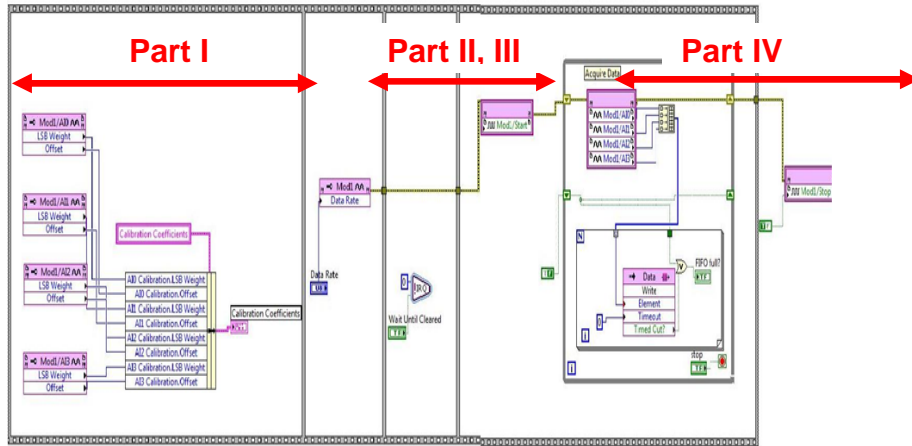


FIGURE 11 Block Diagram of the FPGA Module Showing Data Acquisition From Four Analogue Modules (Part I), Interruption Functions for Synchronizing FPGA and Real-Time Modules (Parts II and III) and the Read and Write Process to DMA FIFO (Part IV).

MODEL BRIDGE FOR TESTING AND CALIBRATING THE SHM SYSTEM

To test and calibrate the designed SHM system and the smart data acquisition system, a model steel bridge was constructed and tested in the Structural Laboratory at UNM. This model bridge used for calibrating the SHM system is shown in Fig. 12. The model bridge is 3.1 m long and 1.1 m wide; it consists of two structural steel trusses. The bridge is divided into three longitudinal traffic lanes spaced at 250 mm each. Underneath the bridge, lateral transverse elements have been used to connect the bottom chord of two trusses.



FIGURE 12 Model Bridge Constructed at UNM Structural Laboratory.

The cross section of connecting members is a 25 mm hollow steel rectangular tube with 1.5 mm thickness. Three 18 mm thick pieces of Plexiglass were used as the bridge deck. Three model trucks made of plastic with rubber wheels were used to model the traffic loading on the bridge. The model trucks have three different weights and weight distributions to realistically simulate traffic. Weights of the trucks were controlled using lead beads of known weights. Additional weights are added to each vehicle by adding bags of lead shot of predetermined weight. Moreover, a CFRP sheet was attached to the bridge deck. Strain gauges were attached to the CFRP sheet to simulate CFRP strengthening that has been used to strengthen the original bridge. The CFRP strip installed on the model bridge with its strain gauge is shown in Fig. 13.

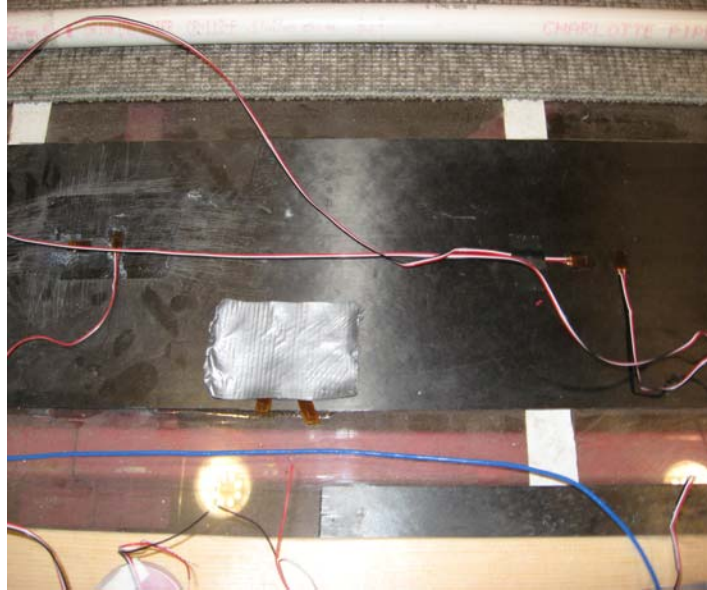


FIGURE 13 CFRP Strip Installed on the Model Bridge Deck with Strain Gauges Installed on the CFRP.

To avoid direct contact between the model truck and the Plexiglass deck, a 5 mm thick carpet was attached on top of the Plexiglass deck. The carpet enables damping of the high frequency spikes produced by direct interaction of truck tires and Plexiglass material. This mimics the interaction between the asphalt layer of real bridges and tires. Using polyvinyl chloride (PVC) tubes, three equally spaced lanes were created on the deck of the model bridge. Moreover, two pieces of wood bolted into the Plexiglass bridge deck were used to attach the accelerometers to top of the bridge. Twenty accelerometers were installed on the prototype bridge. These are the same twenty accelerometers to be installed on Bridge 7937 in Tucumcari. A stainless plate was designed to enable easy installation and replacement of the accelerometers. The same plate will be used to mount the accelerometers on Bridge 7937. The design of the steel plate ensures that there is no vibration at the plate location and excellent fixation to the structure. The accelerometer connection with the steel plate is shown in Fig. 14.

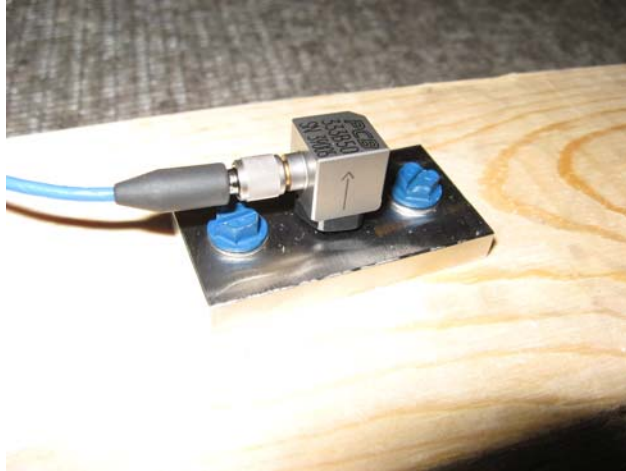


FIGURE 14 Stainless Steel Plate to Mount Accelerometer on the Model and Real Bridge.

The acceleration data was acquired from the model bridge under simulated traffic using the SDA system. Fig. 15 shows a snap shot of the real-time program displaying the acceleration data in real time while monitoring. A display program was developed to present all the monitored accelerations. Fig. 16 presents snap shots of the acceleration data measured at four locations on the model bridge while being monitored.

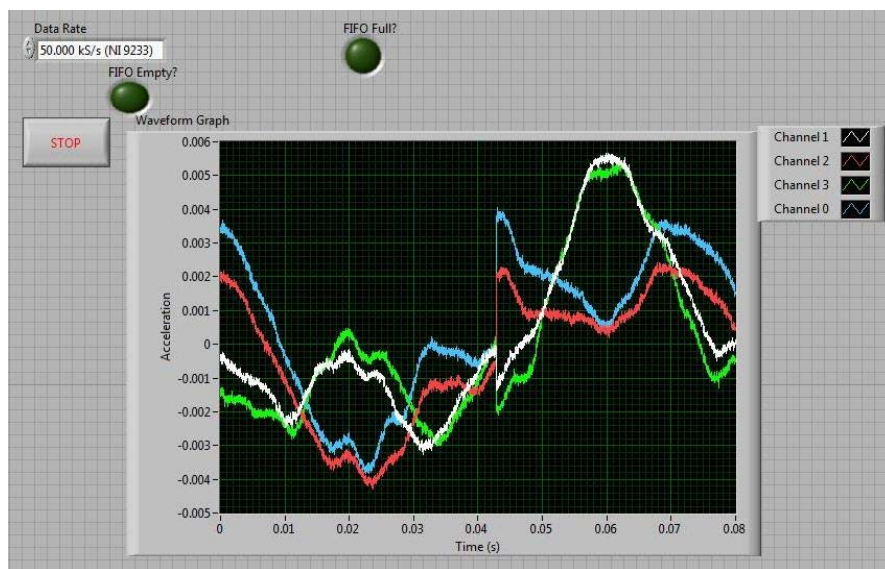


FIGURE 15 Real-Time Acceleration Signals Obtained From the SDA System.

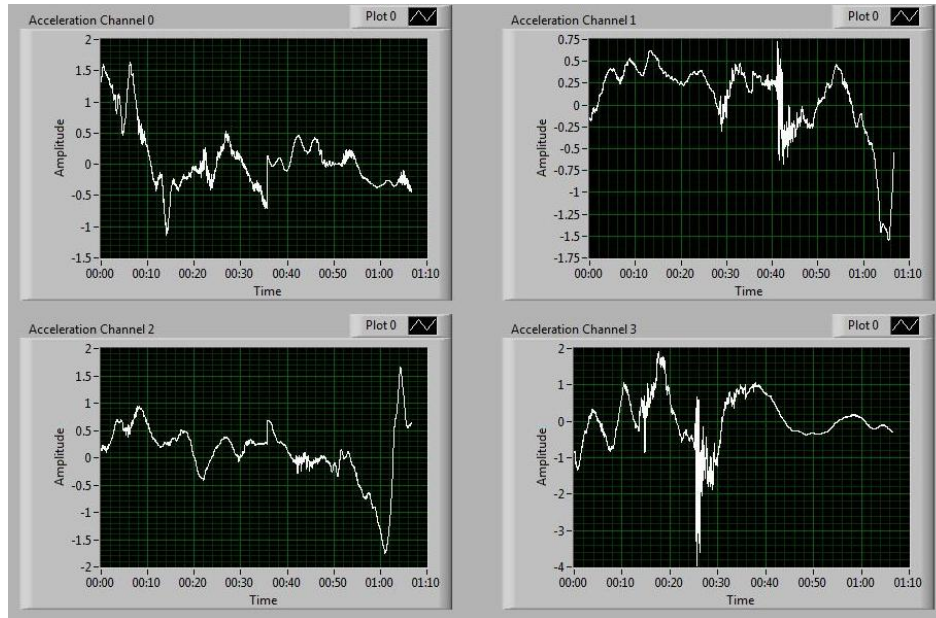


FIGURE 16 Acceleration Signals From Four Different Locations on the Model Bridge.

DAMAGE DETECTION ON THE MODEL BRIDGE

The structural vibration of the model bridge was monitored by recording the accelerations from the twenty accelerometers and strain gauges installed on the bridge. To detect damage occurrence on the bridge, a damage feature will be extracted from the observed acceleration data. This damage feature can then be patterned and damage can be directly related to departure from this pattern. Here, the *Wavelet* method is used for digital signal processing of the acceleration signals. While Fourier transform provides information on the signal in frequency domain, wavelet has the ability to provide information in both time and frequency domains. Using Wavelet Multi Resolution Analysis (WMRA), the original signal can be decomposed to its original components.

Using wavelets, the acceleration signal is decomposed into approximation and detail signals with low and high frequency components, respectively. The wavelet

decomposition provides means to break down the signals into groups of signals at different frequency levels. The decomposed signal of $x'(n)$ at level p can be computed as

$$x'(n) = \sum_{k=-\infty}^{\infty} a_{p,k} \cdot \phi_{p,k}(n) + \sum_{j=1}^p \sum_{k=-\infty}^{\infty} d_{p,k} \cdot \varphi_{p,k}(n) \quad (1)$$

where $x'(n)$ is the decomposed signal. Moreover, $\phi_{p,k}(n)$ and $\varphi_{p,k}(n)$ are the scaling and wavelet basic functions, respectively. The decomposition of the acceleration signal into a group of approximation and details signals is shown schematically in Fig. 17. In this SHM system for Bridge 7937, the scaling and wavelet functions are selected for the *Daubechies db4* mother wavelet. The approximation coefficients $a_{p,k}$ and the detail coefficients $d_{p,k}$ are calculated as

$$a_{p,k} = 2^{(-p/2)} \sum_n x(n) \phi(2^{-p} n - k) \quad (2)$$

$$d_{p,k} = \sum_n x(n) \varphi_{p,k}(n) \quad (3)$$

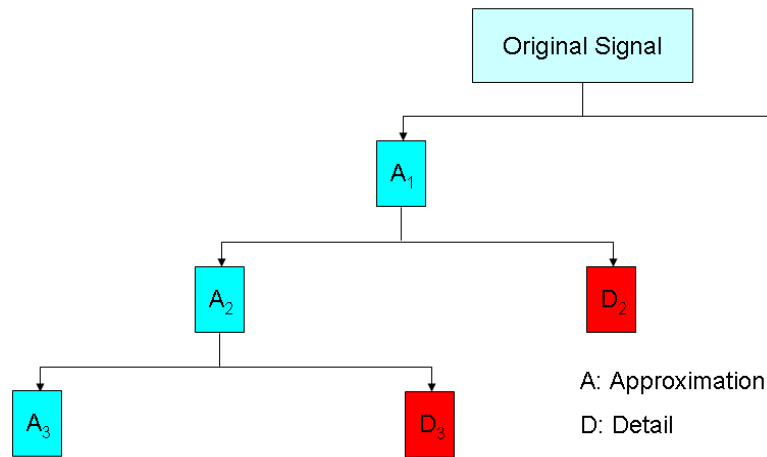


FIGURE 17 Schematic Representation of WMRA Decomposition of the Acceleration Signal.

After decomposing the signal, the third approximation signal (denoted A_3 in Fig. 17) is used to extract the damage feature. The third approximation signal is computed for each accelerometer signal and then the approximation signal is down sized to 500 Hz.

The model bridge was tested by performing traffic load simulation while acquiring data from the bridge using the SDA system to calibrate the SHM system before installation on Bridge 7937 in Tucumcari. Acceleration data was collected for 5 seconds by moving model trucks on the bridge so 3000 data points were extracted for each experiment. Fig. 18 illustrates an example of original acceleration signal obtained from one of the accelerometers along with its third approximation signal denoted A_3 .

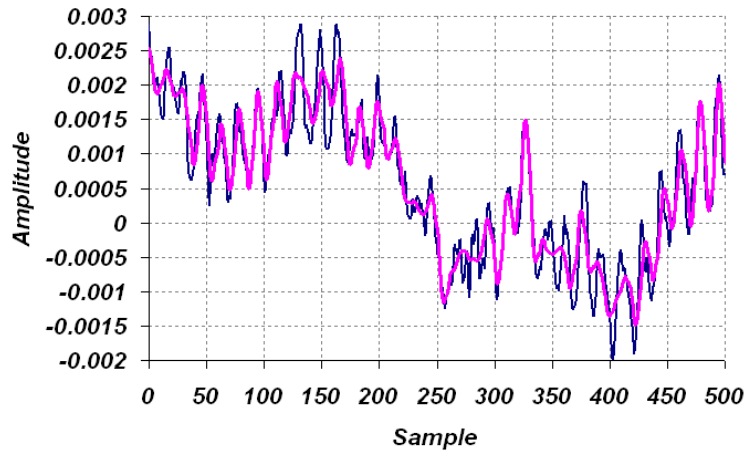


FIGURE 18 Original Acceleration Signal (Blue) Along with its Approximation 3 Signal (Red) Showing the Ability of Wavelet Decomposition to Smoothen the Observed Signal.

Fig. 18 shows that WMRA is capable of removing the noise and all high frequency components from the signal and then down size the sampling rate without changing the original signal. The third resized approximation A_{3R} of the acceleration signal is then used to compute the damage feature as shown in Eq. (4).

$$\lambda = \sum_k (a_{3,k})^2 \quad (4)$$

The damage feature (metric) λ represents the energy of the third approximation signal computed over a time window. Experimental and analytical investigations (4, 8, 9 and 5)

have proven the ability of the proposed damage metric λ to detect and quantify damage occurrence on bridge structures.

To examine the efficiency of the proposed monitoring system, the energy of the third resized approximation signal A_{3R} derived from the acceleration signal at two arbitrary accelerometers at different sides of the bridge was computed for healthy and damage cases. The healthy case is assumed to be the case where all members are attached to each other with completely fixed bolts installed at a specific torque. Damage in the bridge was simulated by removing two diagonal members, one from the first bay of one side and the other from the third bay of the other side. Model trucks were loaded and allowed to move over the bridge simulating traffic in random loading sequence for both the healthy and damage cases. Acceleration signals were recorded for 5 seconds. The signal was divided into thirty time windows, each 166 millisecond wide. The damage metric λ representing the energy of the third resized approximation signal A_{3R} within each time window, was computed following Eq. (4).

A total number of twenty tests for both cases of healthy and damage were performed and thirty values for the damage feature were computed for each test. To be able to compare the healthy and damage performances, the mean value and the standard deviation of the 300 damage feature values collected from two sensors at ten different tests were computed. Assuming that the damage feature (energy of the third resized approximation signal) follows normal probability distribution, the probability of damage feature was computed. Fig. 19 illustrates the probability of damage feature for healthy and damage scenarios computed as one accelerometer.

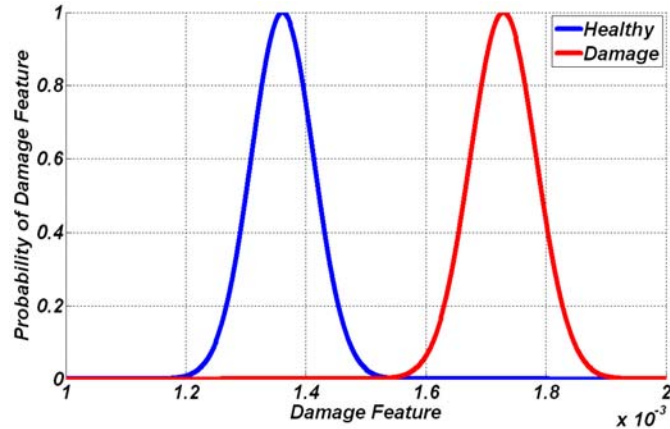
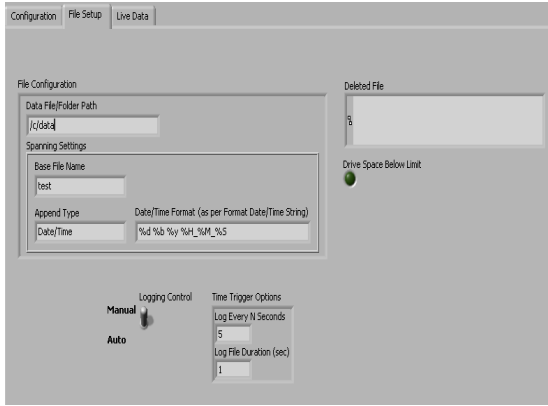
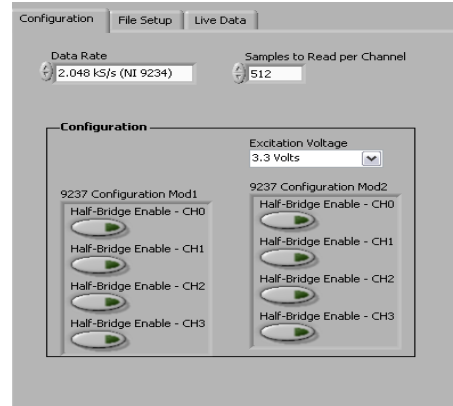


FIGURE 19 Probability of Damage Feature used to Realize Cases of Healthy and Damage Performances at Two Different Sensors Installed on the Prototype Bridge.

It can be observed in this figure that the proposed monitoring system using wavelet domain can easily differentiate between cases of healthy and damage on the prototype bridge. Damage pattern recognition methods (10) can then be used to classify the level of damage in the bridge. The damage feature extraction and pattern recognition algorithms can be used at the host computer level to enable smart SHM. After testing all sensors, the proposed SDA and all sensors were decided to be working as designed. Experiments were also performed for data communication over the worldwide web for all sensor data. Snap shots of the SHM web-based software developed for data control and data transfer is shown in Fig. 20. Moreover, a webpage for enabling data observation and data transfer via file transfer protocols (FTP) was developed. A snap shot of this webpage is shown in Fig. 21. The web page and the FTP system were tested and proved capable of communicating the data observed from the model bridge.



(a)



(b)

FIGURE 20 Web Tools Developed for (a) Data Transfer from the Bridge and (b) Data Rate and Sensor Selection Control on the SDA.

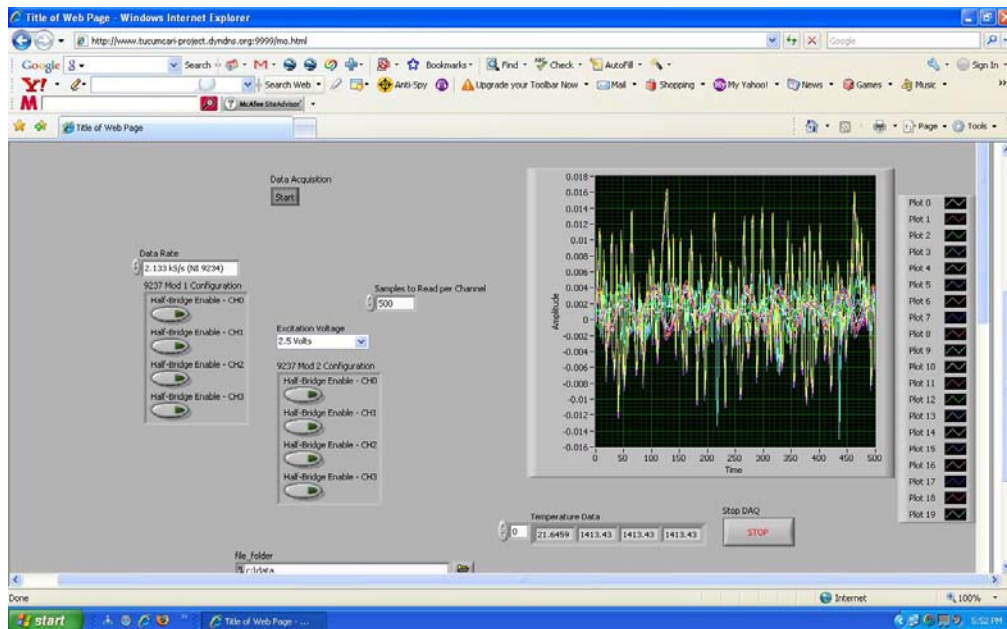


FIGURE 21 Snap Shot of the Webpage Developed for Efficient Data Transfer Using the Worldwide Web.

DESIGN OF PHOTOVOLTAIC POWER SYSTEM FOR SMART SHM

Installation of an SHM system at a remote location such as Bridge 7937 in Tucumcari necessitated the development of an innovative method to power the system. After careful investigation, it was found that there was no electrical power availability at the bridge site. Therefore, the researchers decided that a photovoltaic (PV) system would need to be

designed in order to provide the power energy required to enable efficient SHM. The geographical position of the city of Tukumcari, New Mexico was defined at Latitude: 35° 10' 18" N and Longitude: 103° 43' 27" W. The PV system design consists of estimating the energy load required followed by an estimate of autonomy system requirements for backup., Finally, a layout analysis of the proposed PV system and the structural system to support the solar panels are presented.

Electrical Load Estimate

In order to design a proper PV system for solar energy, the required energy load for the SDA system on Bridge 7937 was estimated. The PV system needs to support the wireless communication modem, the SDA system, current inverter device and a time controller. Based on the operation requirements of 8 hours of continues energy supply, the following daily energy consumption (E_c) was estimated.

TABLE 2 Energy Consumption Estimation for Powering the SHM System at Bridge 7937 in Tukumcari, New Mexico.

Device	Power (W)	Daily Operation time (hr)	Daily Consumption (Whr)
Wireless Modem	4.2	8	33.6
DAQ module	48	8	384
Inverter	7.8	8	62.4
Time controller	1.4	24	33.6
<i>E_c (Whr/day)</i>			513.6

Energy Autonomy

The energy source (in this case solar energy) is not available continuously; therefore, an energy autonomy or energy backup method had to be designed. The most common method is an electrical battery system, which will be installed at this project. The battery

system has to be able to satisfy all the energy demands in the data acquisition system for some autonomy time required by the specifications of the design. For this particular case, three days of autonomy time was assumed. The battery capacity for holding energy is rated in amp-hours and the energy capacity for the battery system (E_b) can be calculated according to the energy demand as

$$E_b = \frac{E_c \varepsilon_l D_A}{b r \varepsilon_b (1 - \alpha_w)} \quad (5)$$

Where ε_l is the inverters efficiency, b is the battery system voltage, r is the discharge cycle rate, ε_b is the battery's efficiency, α_w is the wiring losses and D_A is the autonomy time in days. Using the energy consumption data calculated in the electrical load estimation and the battery system parameter specified in Table 3,

TABLE 3 Battery System Parameters.

b	12 V
r	60%
ε_b	90%
ε_i	95%
α_w	2%

the energy capacity for different battery systems for different autonomy days can be calculated as

$$E_b = \frac{513.6 * 0.95 * 1}{12 * 0.6 * 90 * (1 - 0.2)} = 76.8 \text{ Ahr} \quad (6)$$

PV Array Design

Once the estimation of the energy demand for the system was determined, the photovoltaic arrays characteristics, dimensions and arrangement could be computed to satisfy the energy consumption and backup system. Since PV systems depend on solar

energy, the sun hours observed during the day was an essential parameter to calculate the PV array. For this specific system, the location of the system is below the Tucumcari bridge at Latitude: $35^{\circ} 10' 18''$ N - Longitude: $103^{\circ} 43' 27''$ W in a fixed array configuration experiencing morning shadowing as shown in Fig. 22.

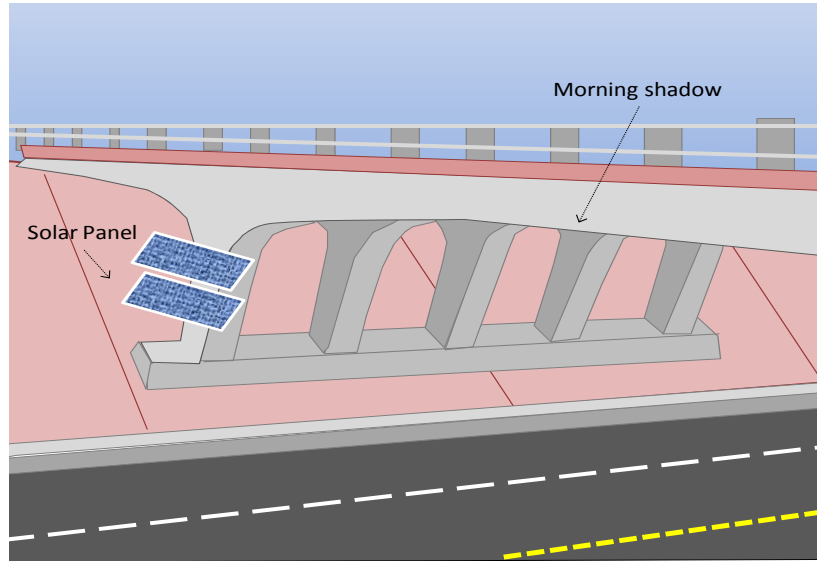


FIGURE 22 PV System Location (Tucumcari Latitude: $35^{\circ} 10' 18''$ N - Longitude: $103^{\circ} 43' 27''$ W) and the Proposed Location of Solar Panels to Enable SHM Power.

Based on an average sun tracking system as shown in Fig. 23, the PV system configuration suggested in Fig. 22 should be able to provide an estimated average peak sun hours (h_s) of 5 hours during the entire year.

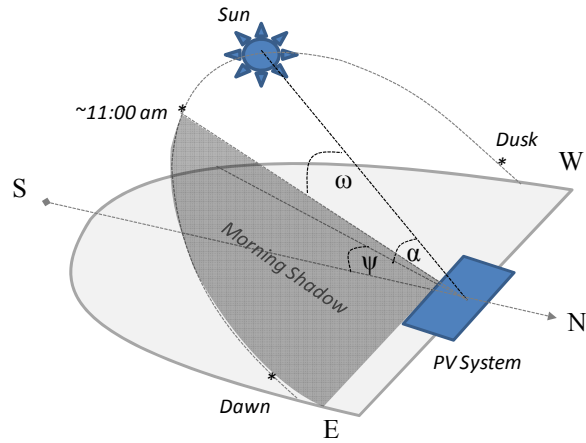


FIGURE 23 PV System Sun Tracking Schematic.

The angle α in Fig. 23 represents the altitude of the sun at a specific season of the year expressed in degrees, ψ is the azimuth angle and ω is the time angle expressed in degrees with respect to a specific time/hour of the day. Once the average peak sun hours are estimated for the SHM system, the PV array power required can be computed as

$$P_{array} = \frac{E_b b}{h_s \alpha_T \beta \varepsilon_I} \quad (7)$$

Where α_T is the temperature loss factor, β is the Derate factor and ε_I is the inverted efficiency factor. The PV array power required to satisfy the different autonomy days can be calculated as

$$P_{array} = \frac{76.8 * 12}{5 * 0.88 * 0.84 * 0.95} = 262.6 W \quad (8)$$

Charge Controller

In order to have good management of energy resources in the PV system, a charge controller was incorporated in the system. A charge controller is able to make the system operate at the optimum solar panels energy absorption by performing the maximum power point tracker (MPPT). This controller will also limit the rate at which electrical current is either added to or drawn from the electric batteries. It prevents overcharging and may prevent against over voltage, which can reduce battery performance and/or lifetime.

The adequate charge controller had to be designed according to the PV panel array power and the autonomy battery system previously calculated. These parameters determine the charge controller capacity and parameters that satisfy the system. Based on the PV array power, the solar panel specifications for Kyocera KC130TM 130 Watts Solar Panel and the energy capacity and battery sizing calculated in previous sections, the charge controller should satisfy the energy requirements. The design indicated a 20 controller array Amp and 5.1 controller load Amp.

Time Controller

In PV systems, energy consumption and management is an important issue due to the lack of full accessibility to sun energy radiation. Therefore, energy consumption has to be controlled to avoid energy waste by powering equipment when it is not needed. Programmable time controls are among the most effective energy management devices available. Battery re-chargers and other types of equipment can be effectively managed with time controls.

The SDA system is the main source of the load to be supported by the PV system. Therefore, optimized energy management should be carried out to power the system only when data acquisition is required and avoided when powering equipment is not needed. Programmable time controllers are utilized in the project as a means of energy management device. The time controller used here has the ability to set multiple on/off operations, and includes the ability to have different schedules for each day of the week. Due to the different uploading and downloading of traffic at different times to the wireless communication device, a feasible operation time for the data acquisition system has been determined as shown in Table 4.

TABLE 4 Time Controller Schedule for the PV System for Bridge 7937.

	Monday	Tuesday	Wednesday	Thursday	Friday	Saturday	Sunday
2:00 am	Off	Off	Off	Off	Off	Off	Off
4:00 am	Off	Off	Off	Off	Off	Off	Off
6:00 am	On	On	On	On	On	On	On
8:00 am	On	On	On	On	On	On	On
10:00 am	On	On	On	On	On	On	On
12:00 pm	Off	Off	Off	Off	Off	Off	Off
2:00 pm	Off	Off	Off	Off	Off	Off	Off
4:00 pm	Off	Off	Off	Off	Off	Off	Off
6:00 pm	On	On	On	On	On	On	On
8:00 pm	On	On	On	On	On	On	On
10:00 pm	On	On	On	On	On	On	On
12:00 am	Off	Off	Off	Off	Off	Off	Off

System Layout

Based on the respective designs of the various components of the PV system calculated in previous sections, a layout schematic of the proposed PV system could be created.

Fig. 24 shows such schematic of the proposed PV system.

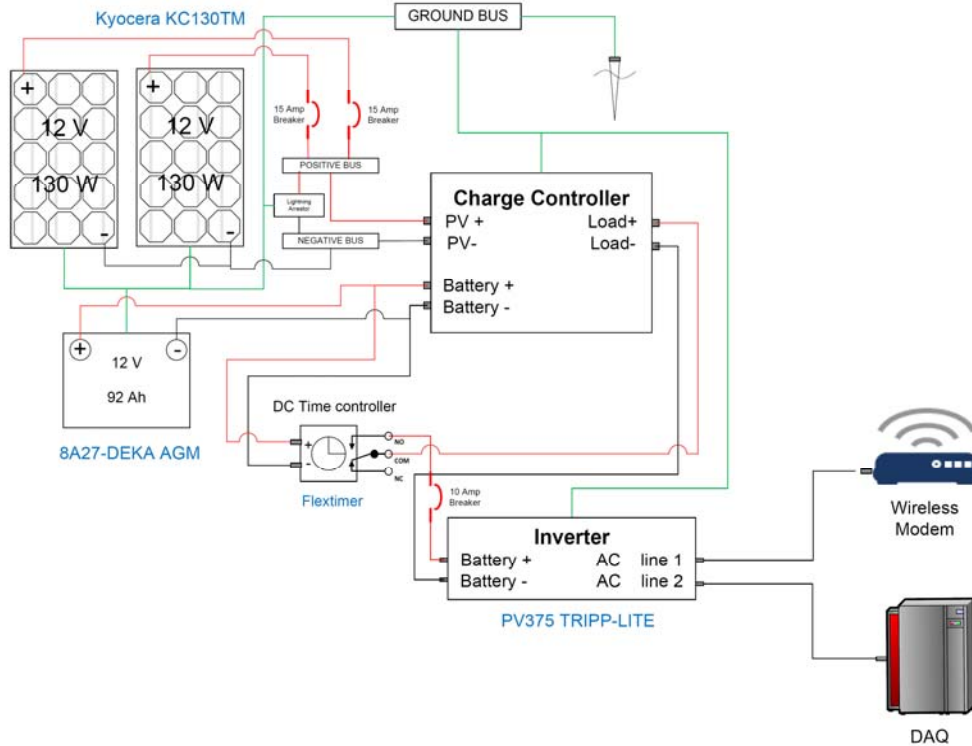


FIGURE 24 Layout of Proposed PV System for 1 Day of Autonomy.

The different energy demands and PV capacities for the system shown in this schematic can be satisfied with different components. Brands, capacities and qualities vary between manufacturers and different PV system configurations with distinct components can be found to satisfy the same system capacities in discourse. For this particular case, the system was designed over the inverter type 375 Watt TRIPP-LITE, the battery system utilized battery type 8A27-DEKA AGM, and the PV array utilized the solar panel Kyocera KC130TM. The structural system to support the solar panels and attaching them to the bridge structure is shown in Fig. 25.

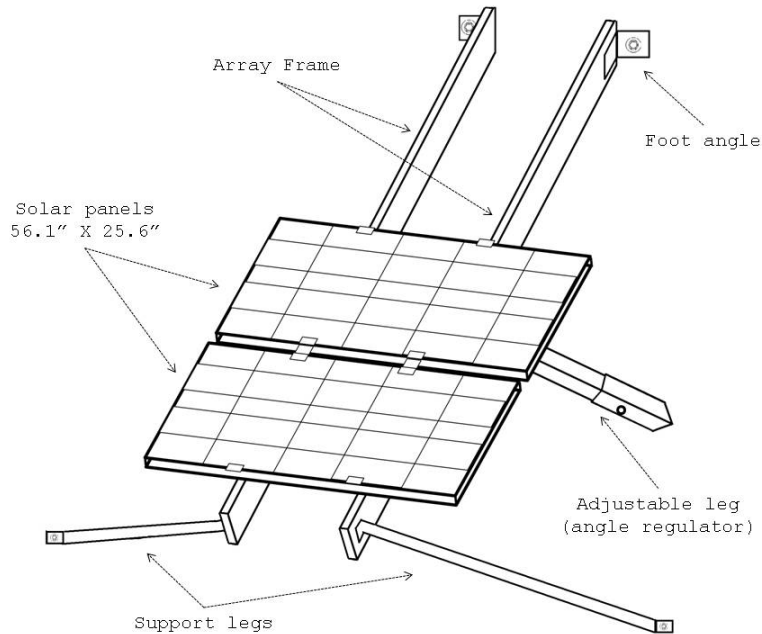


FIGURE 25 Structural System to Support Solar Panels and Attach Them to The Bridge

CONCLUSION

This report describes the design of the new structural health monitoring system to monitor Bridge 7937 in Tucumcari New Mexico. The new SHM system is vibration-based designed to detect damage in the bridge structure by realizing changes in structural vibration. The new system includes 20 accelerometers, 8 strain gauges and 4 thermocouples. The system is designed to work remotely and to transfer the data using wireless protocols with no need to visit the bridge site. The new system shall allow continuous observations of the bridge structure ensuring its safety for public use.

REFERENCES

1. AASHTO *LRFD Bridge Design Specifications, Manual for Condition Evaluation of Bridges*. American Association of State Highway and Transportation Officials. 2006 Interim revisions, Second Edition, Washington, D.C, 2006.
2. Neild, S.A., P.D. McFadden and M.S. Williams. A Review of Time-Frequency Methods for Structural Vibration Analysis. *Engineering Structures*, Vol. 25, 2003, pp. 713-728.
3. Li, H., J. Ou, X. Zhao, W. Zhou, H. Li and Z. Zhou. Structural Health Monitoring System for the Shandong Binzhou Yellow River Highway Bridge. *Computer-Aided Civil and Infrastructure Engineering*, Vol. 21, 2006, pp. 306-317.
4. Reda Taha, M., A. Noureldin, A. Osman and N. El-Sheimy. Introduction to the Use of Wavelet Multi-Resolution Analysis for Intelligent Structural Health Monitoring. *Canadian Journal of Civil Engineering*, Vol. 31, No. 5, 2004, pp. 719-731.
5. Azarbajejani, M., A. El-Osery, K.-K. Choi and M.M. Reda Taha. Probabilistic Approach for Optimal Sensor Allocation in Structural Health Monitoring. *Smart Materials and Structures*, Vol. 17, No. 5, 2008, paper # 055019.
6. Mehrani, E. and A. Ayoub. Evaluation of Fiber Optic Sensors for Remote Health Monitoring of Bridge Structures. *Smart Structures and Systems*, Vol. 5, No. 4., 2009.
7. Shrive, P.L., J.P. Newhook, T.G. Brown, N.G. Shrive, G. Tadros and J. Kroman. Thermal Strains in Steel and Glass Fibre Reinforced Polymer Reinforcement in a Bridge Deck. In *Proceedings of the International Conference on Performance of Constriction Materials (ICPCM)*, El-Dieb et al. Eds., Cairo, Egypt, Vol. 1, 2003, pp. 429-437.
8. Horton, S., M.M. Reda Taha and T. J. Baca. A Neural-Wavelet Damage Detection Module for Structural Health Monitoring. In *Proceedings of International Workshop on Structural Health Monitoring*, Chang, Fu-Kuo, Ed., Stanford, USA, 2005, pp. 556-564.
9. McCuskey, M., M.M. Reda Taha, S. Horton and T.J. Baca. Identifying Damage in ASCE Benchmark Structure using a Neural-Wavelet Module. In *Proceedings of the International Workshop on Structural Health Monitoring*, Granada, Spain, July 2006, pp. 421-428.
10. Reda Taha, M.M. and J. Lucero. Damage Identification for Structural Health Monitoring using Fuzzy Pattern Recognition. *Engineering Structures*, Vol. 27, No. 12, 2005, pp. 1774-1783.



New Mexico Department of Transportation
RESEARCH BUREAU
7500B Pan American Freeway NE
PO Box 94690
Albuquerque, NM 87199-4690
Tel: (505) 841-9145

NEW MEXICO DEPARTMENT OF TRANSPORTATION

RESEARCH BUREAU

Innovation in Transportation

Monitoring Long-Term In-Situ Behavior of Installed Fiber Reinforced Polymer:

Report III: Analysis and Results of Post-Construction
Monitoring for Bridge 7937 in Tucumcari

Prepared by:
University of New Mexico
Department of Civil Engineering
Albuquerque, New Mexico 87131

Prepared for:
New Mexico Department of Transportation
Research Bureau
7500-B Pan American Freeway NE
Albuquerque, New Mexico 87109

In Cooperation with:
The US Department of Transportation
Federal Highway Administration

**Report
NM08TT-02**

JUNE 2009

1. Report No. NM08TT-02		2. Government Accession No.		3. Recipient's Catalog No.	
4. Title and Subtitle Monitoring Long-Term In-Situ Behavior of Installed Fiber Reinforced Polymer Report III: Analysis and Results of Post-Construction Monitoring for Bridge 7937 in Tucumcari.				5. Report Date June 2009	
				6. Performing Organization Code	
7. Author(s) M. M. Reda Taha, M. Azarbayejani				8. Performing Organization Report No.	
9. Performing Organization Name and Address University of New Mexico Department of Civil Engineering Albuquerque, NM 87131				10. Work Unit No. (TRAIS)	
				11. Contract or Grant No. CO5102	
12. Sponsoring Agency Name and Address Research Bureau New Mexico Department of Transportation 7500-B Pan American Freeway NE Albuquerque, NM 87109				13. Type of Report and Period Covered	
				14. Sponsoring Agency Code	
15. Supplementary Notes					
16. Abstract The objective of this report is to provide information on the installation and operation of the new structural health monitoring (SHM) system installed on Bridge 7937 in Tucumcari, New Mexico. The new SHM system is based on field programmable gated array (FPGA) technology and operates using wireless communication. This report also describes the installation of solar panels used to power the SHM system with renewable energy. New software specially designed for data analysis and damage detection of Bridge 7937 is described. The new SHM system hardware and software are operational and provide smart monitoring of Bridge 7937 for public safety.					
17. Key Words: Structural health monitoring, Wireless monitoring, AASHTO LRFD, Fiber reinforced polymers.			18. Distribution Statement Available from NMDOT Research Bureau		
19. Security Classif. (of this report) None		20. Security Classif. (of this page) None		21. No. of Pages 30	22. Price

**MONITORING LONG-TERM IN-SITU BEHAVIOR OF INSTALLED
FIBER REINFORCED POLYMER**

**Report III: Analysis and Results of Post-Construction Monitoring for
Bridge 7937 in Tucumcari**

by

M. M. Reda Taha
M. Azarbayejani
University of New Mexico
Department of Civil Engineering

Prepared for:
New Mexico Department of Transportation, Research Bureau

A Report on Research Sponsored by:
New Mexico Department of Transportation, Research Bureau

In Cooperation with the
U.S. Department of Transportation, Federal Highway Administration

June 2009

NMDOT, Research Bureau
7500-B Pan American Freeway NE
Albuquerque, NM 87109

PREFACE

The purpose of this report is to present the installation and field implementation of an innovative structural health monitoring (SHM) system designed to provide continuous monitoring of Bridge 7937 in Tucumcari, New Mexico. Bridge 7937 was previously strengthened using carbon fiber reinforced polymer (CFRP) sheets as a showcase strengthening project. The new SHM system is installed and is currently operational. The new system is powered by clean solar energy. New software specially designed for analyzing monitoring data observed using the new SHM system is described. The new SHM of Bridge 7937 allows smart monitoring of the bridge structure for public safety.

NOTICE

The United States Government and the State of New Mexico do not endorse products or manufacturers. Trade or manufacturers' names appear herein solely because they are considered essential to the object of this report. This information is available in alternative accessible formats. To obtain an alternative format, contact the NMDOT Research Bureau, 7500-B Pan American Freeway NE, Albuquerque, NM 87109 (PO Box 94690, Albuquerque, NM 87199-4690) or by telephone (505) 841-9150.

DISCLAIMER

This report presents the results of research conducted by the author(s) and does not necessarily reflect the views of the New Mexico Department of Transportation. This report does not constitute a standard or specification.

ABSTRACT

The objective of this report is to provide information on the installation and operation of the new structural health monitoring (SHM) installed on Bridge 7937 in Tucumcari, New Mexico. The report describes the components of the new SHM system and the steps of installation. The new SHM system is based on field programmable gated array (FPGA) technology and operates using wireless communication. This report also describes the installation of the solar panels used to power the SHM system with clean energy.

New software specially designed for data analysis and damage detection of Bridge 7937 using the vibration data acquired using the SHM system is described. The ability of the software to record the bridge history and to analyze remotely observed data for damage detection is explained. The new SHM system provides innovative approach and techniques for monitoring the nation aging infrastructure. The new SHM system is currently operational and provides smart monitoring of Bridge 7937 for public safety.

ACKNOWLEDGMENTS

This work is funded by Federal Highway Administration (FHWA) Contract Number CO5102 to New Mexico Department of Transportation (NMDOT) through the Innovative Bridge Research and Deployment (IBRD) program. The authors greatly acknowledge this support. Technical help during design and installation of the SHM system by System of Systems LLC., National Instruments, Inc. and 3B Builders, Inc. is greatly acknowledged. Field support and excellent cooperation from NMDOT District 4 Engineer “Heather Sandoval” and her field crew is highly appreciated.

TABLE OF CONTENTS

PREFACE	III - i
ABSTRACT	III - ii
ACKNOWLEDGMENTS	III - iii
TABLE OF CONTENTS	III - iv
FIGURES	III - v
OBJECTIVE	III - 1
BRIDGE DESCRIPTION	III - 1
STRUCTURAL HEALTH MONITORING OF BRIDGE 7937	III - 3
INSTALLATION OF SHM SYSTEM ON BRIDGE 7937	III - 5
USER INTERFACE TO MONITOR BRIDGE 7937	III - 14
DATA ANALYSIS FOR DAMAGE DETECTION	III - 20
CONCLUSION.....	III - 29
REFERENCES.....	III - 30

FIGURES

Fig. 1 Bridge 7937 at Tucumcari	III - 2
Fig. 2 K-Frames of Bridge 7937	III - 2
Fig. 3 FRP Sheets Installed on Bridge 7937	III - 3
Fig. 4 3D Finite Element Model for Bridge 7939 Used to Identify Critical Bridge Locations	III - 4
Fig. 5 Schematic Representation of SHM System Showing all its Components as Designed for Bridge 7937	III - 5
Fig. 6 Installing of the Steel Box to House All Electrical Components at the Bottom of Bridge 7937	III - 6
Fig. 7 Steel Box Used for Housing the Data Acquisition System and All SHM Components	III - 6
Fig. 8 Installation of Hangers Underneath the Girders of the Bridge Using Tapcon Bolts	III - 7
Fig. 9 (a) Accelerometer attached to stainless steel plate before installation. (b) An accelerometer attached to the bridge slab using a stainless steel plate .	III - 8
Fig. 10 (a) View of the Bridge After Installation of all Accelerometers. (b) All Accelerometers Wiring Going to the Box. Figure Also Shows the Wireless Antenna	III - 9
Fig. 11 Electrical Boxes and Conduits to Pass Power to the SDAQ Using the Solar Panels	III - 10
Fig. 12 Weights Applied on Top of Each Installed Strain Gauge	III - 11
Fig. 13 Covered Strain Gauges Attached to the FRP Sheets	III - 11
Fig. 14 All the Strain Gauges After Being Installed on the FRP Sheets and Connected to the Wires Transmitting the Strain Signals to the Data Acquisition (DAQ) Device	III - 12
Fig. 15 Concrete Casting Over Area of Bridge Deck Strengthened with FRP ...	III - 12
Fig. 16 Top of Bridge Deck After Concrete Casting Showing the Connection of the Sensors to the Monitoring Box Under the Bridge	III - 12
Fig. 17 One Thermocouple Sensor Attached to the Web of the Bridge Girder	III - 13
Fig. 18 Data Acquisition System, Rechargeable Batteries, Power Inverter, Digital Timer Switch and the Wireless Modem Located at the Steel Box .	III - 14
Fig. 19 Solar Power System Installed on Bridge 7937 to Provide Clean Renewable Energy for The SHM System	III - 15

Fig. 20 Solar Power System Installed on Bridge 7937 to Provide Clean Renewable Energy for The SHM System	III - 15
Fig. 21 Graphical User Interface Shows the “Configuration” of Modules	III - 16
Fig. 22 Graphical User Interface Shows “File Setup”	III - 17
Fig. 23 Graphical User Interface Shows “Live Data”	III - 18
Fig. 24 Live Data From the Web Address to View Bridge 7937 Recorded on June 26, 2009 (a) Acc 1 & (b) Acc 9	III - 19
Fig. 25 FTP Graphical Interface for Transferring the Data from SDAQ	III - 20
Fig. 26 Snapshot of SMART-SHM-START Software Shows the Four Views That a User Can Display Synchronized Data in Them Along With the Temperature	III - 21
Fig. 27 Raw Data Collected From Four Different Sensors With the Temperature Data as Shown in SMART-SHM-START Software	III - 22
Fig. 28 SMART-SHM-START software shows raw data, Fourier transform, Wavelet transform and decimated Wavelet signals collected from sensor 8 installed on the bridge. The bottom row shows the temperature at four locations on the bridge	III - 23
Fig. 29 Snapshot of SHM-SMART-DAMAGE Software Designed for Observing Bridge Behavior and its Change Over Time	III - 24
Fig. 30 Snapshot of SMART-SHM-Damage Shows the History of the Frequency Damage Feature at Sensor 1 as Extracted From Bridge 7937 .	III - 27
Fig. 31 Snapshot of SMART-SHM-Damage Show the History of the Wavelet Damage Feature at Sensor 8 as Extracted From Bridge 7937	III - 28

OBJECTIVE

The objective of this report is to report on installation and testing of the innovative structural health monitoring (SHM) system on bridge 7937 in Tukumcari, New Mexico. The post processing software designed to analyze the data acquired from the bridge will also be explained in detail describing how the SHM system is planned to monitor the bridge continuously and remotely. Moreover, different analyses are presented to extract features from the structural acceleration signals obtained from the bridge that could differentiate between healthy and damage states of the bridge.

BRIDGE DESCRIPTION

Bridge 7937 on Interstate 40 (I-40) in the city of Tukumcari, New Mexico was selected for implementation of the monitoring system. As shown in Figs. 1 and 2, the bridge consists of five reinforced concrete (RC) K-Frame girders. The K-Frames form three spans; 42 ft, 104 ft and 42 ft. Each K-frame has a rectangular RC cross-section whose depth varies along the length of the bridge. Asphalt overlay is used on the top of bridge 7937. Moreover, the longitudinal and transverse reinforcements vary along the length of the bridge. Fig. 3 illustrates the cross-section and the longitudinal and transverse reinforcements of this bridge.

During the last two decades since the bridge was constructed, the size and weight of trucks passing over I-40 have increased dramatically. It is expected that the moment and shear demand of the current traffic load might exceed bridge capacity (1). Previous research by the University of New Mexico (UNM) team showed that the bridge does not have sufficient capacity in negative moment region according to AASHTO 2006. To ensure that bridge 7937 falls within the state limit requirements of AASHTO code, UNM

researchers installed four fiber reinforced polymer (FRP) strips on the bridge in summer 2007. Fig. 3 shows FRP strips installed on bridge 7937 by the UNM team.



FIGURE 1 Bridge 7937 at Tucumcari.



FIGURE 2 K-Frames of Bridge 7937.



FIGURE 3 FRP Sheets Installed on Bridge 7937.

STRUCTURAL HEALTH MONITORING OF BRIDGE 7937

The structural health monitoring (SHM) system to monitor bridge 7937 includes accelerometers and strain gauges along with thermocouples. Twenty accelerometers were used to extract structural dynamic information at different locations on the bridge. The acceleration data was used to extract damage feature(s) which can differentiate between healthy and damage conditions and enable warnings when the bridge is damaged. The SHM system for bridge 7937 was designed to operate using a field programmable gate array (FPGA) data acquisition system as reported in Report 2. This system is denoted as smart data acquisition system (SDAQ) for its capability to connect wirelessly to the Worldwide Web and transfer synchronized monitoring data from different sensors using HTTP and FTP protocols.

The location of the sensors was determined based on structural analysis of the bridge by identifying the most critical structural locations. A three-dimensional finite element model of the bridge is shown in Fig. 4. This model was used to simulate the structural behavior of the bridge and therefore to determine the critical bridge locations that are

more prone to damage. This information was used to identify the sensor locations using different approaches as described in Report 1 (2).

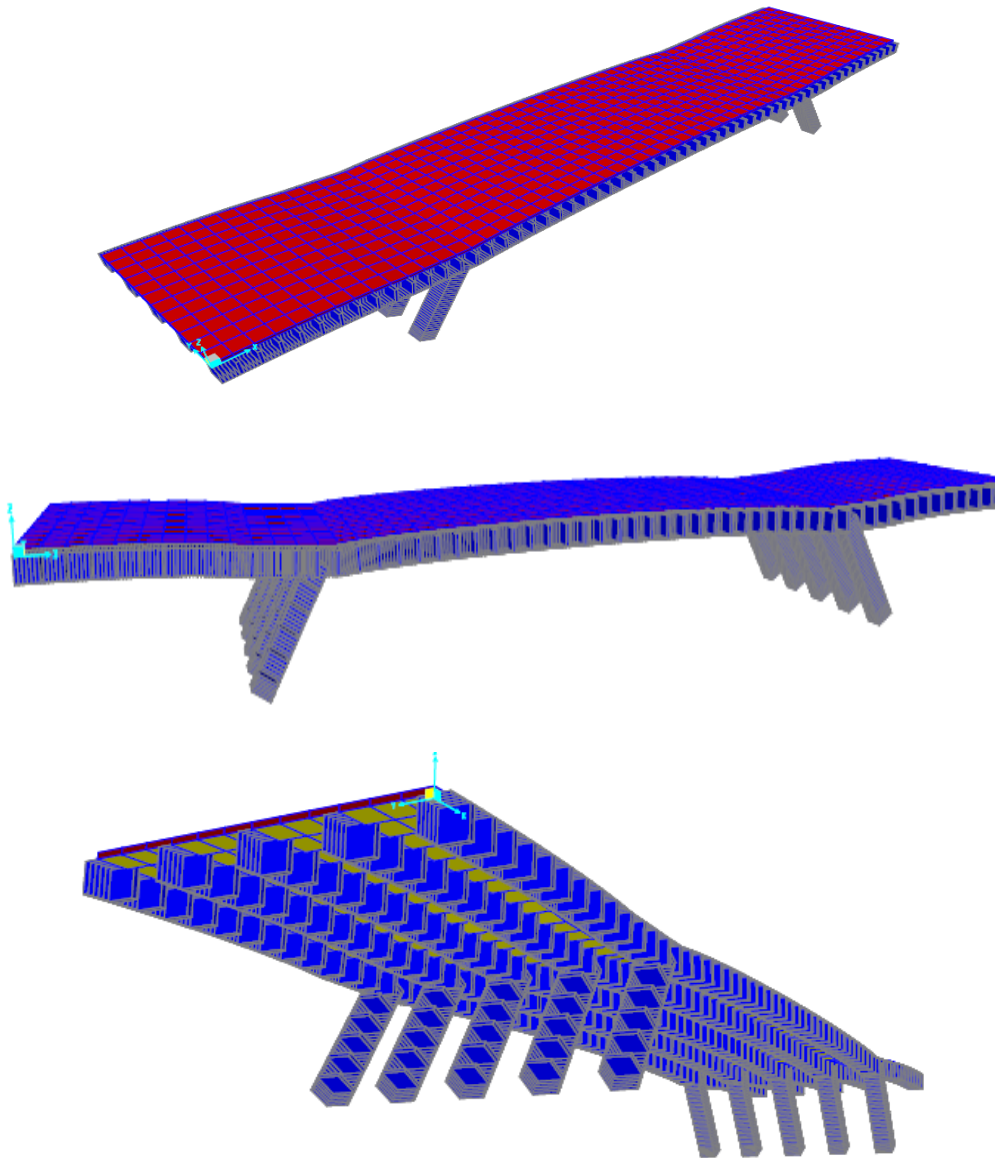


FIGURE 4 3D Finite Element Model for Bridge 7939 Used to Identify Critical Bridge Locations.

Moreover, strain gauge sensors were used on FRP sheets to monitor the possible debonding between FRP sheets and concrete deck of the bridge. Thermocouples were used in different locations at top and bottom of the bridge to measure temperature and

determine temperature gradient. Fig. 5 illustrates a schematic of the SHM system installed on bridge 7937 and all its components. Fig. 5 also shows the wireless communication designed for the bridge and how it is supposed to operate.

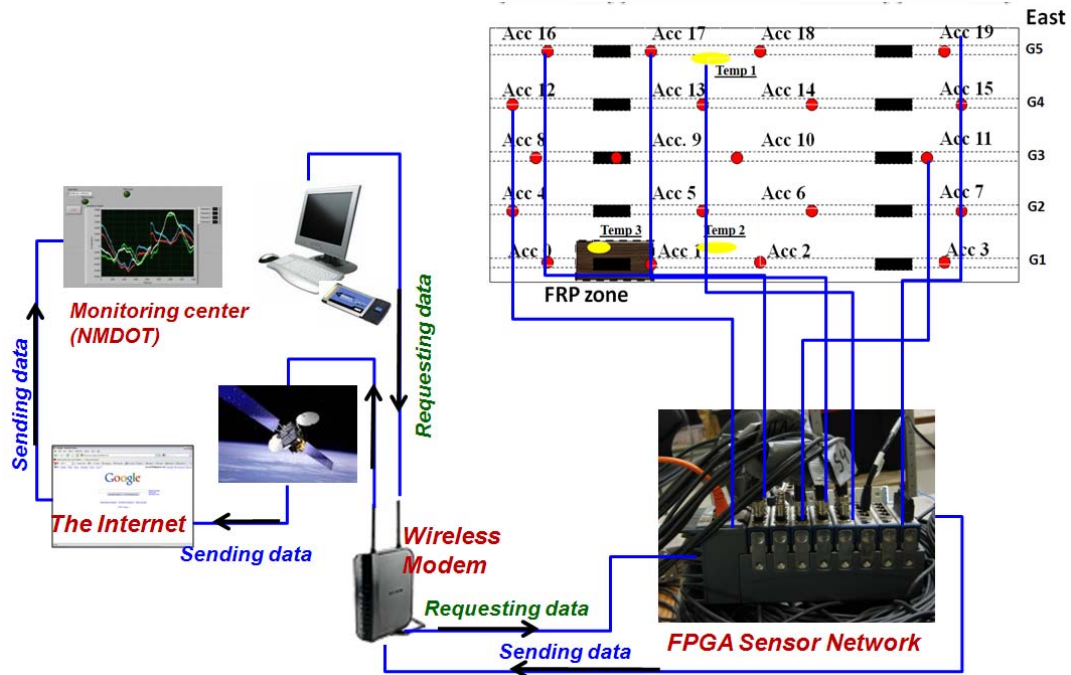


FIGURE 5 Schematic Representation of SHM System Showing all its Components as Designed for Bridge 7937.

INSTALLATION OF SHM SYSTEM ON BRIDGE 7937

After testing and calibrating all the components of SHM system on a model truss bridge in UNM laboratory and ensuring system ability to detect damage, the SHM system was brought to the bridge location in Tucumcari and was installed on bridge 7937. Installation of the SHM system was performed by UNM SHM research group who authored this document and 3B Builders who are a certified electrical contractors operating in New Mexico.

The first step was to install a steel box for housing all the data acquisition, wireless modem and other electronic devices such as power inverter and solar panel batteries. The

steel box is outdoor rated enclosure (Nema 4) that has two holes on top to connect all the wires into the system. Figs. 6 and 7 show the installation process as well as a photograph of the inside of the steel box before installation of the SHM components. As shown in Fig. 6 the steel box was installed on the third K-Frame underneath the bridge.

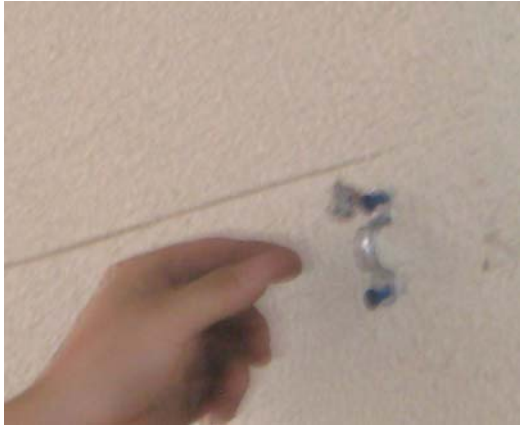


FIGURE 6 Installing of the Steel Box to House All Electrical Components at the Bottom of Bridge 7937.



FIGURE 7 Steel Box Used for Housing the Data Acquisition System and All SHM Components.

After installation of the steel box on the bridge, hangers were drilled into the bridge and attached using tapcon screws to make a path for accelerometer cables into the steel box as shown in Fig. 8.



(a)



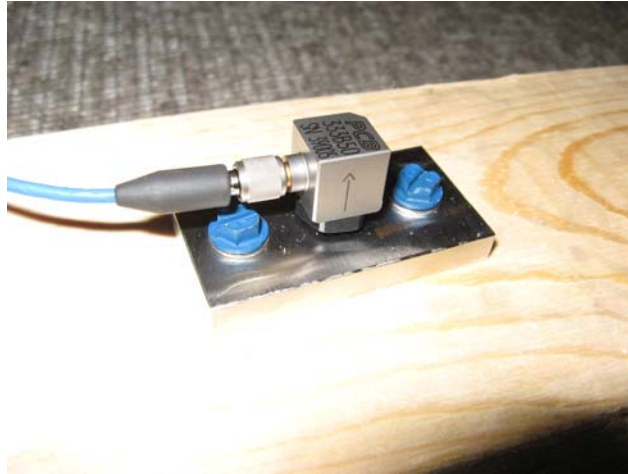
(b)

FIGURE 8 Installation of Hangers Underneath the Girders of the Bridge Using Tapcon Bolts.

By putting enough hangers on each girder of the bridge and connecting wires through the hangers, accelerometers were installed using stainless steel plates that were specially designed and tested before installation in the UNM Structures Laboratory as described in Report 2. The stainless steel plates were anchored to the bottom of the bridge deck in very close proximity to the girders, and then the accelerometers were attached to the steel plates.

After the accelerometers were attached to the stainless plates, a silicon insulator was installed over the sensor and the stainless steel plate to produce a silicon dome over the accelerometer to environmentally protect the sensor against dust and all other harsh environmental effects. Fig. 9 illustrates the original stainless steel plates and the accelerometers before installation on the bridge and the protected accelerometers with silicon dome after being installed on the bridge with the stainless steel plate. Fig. 10

shows a view of the bridge where after all the accelerometers were installed and wired to the steel box. In this figure, the wireless antenna can be observed.



(a)



(b)

FIGURE 9 (a) Accelerometer attached to stainless steel plate before installation. (b) An accelerometer attached to the bridge slab using a stainless steel plate.



(a)



(b)

FIGURE 10 (a) View of the Bridge After Installation of all Accelerometers. (b) All Accelerometers Wiring Going to the Box. Figure Also Shows the Wireless Antenna.

Two conduits with two small electrical boxes were made, one to pass the cables from the solar panel to the steel box housing all the data acquisition system to power the SDAQ, and the other to pass the cables from strain gauges attached on the FRP zone on top of the bridge to the data acquisition (DAQ) box at the bottom. Fig. 11 shows these conduits and the electrical box made to house the electrical cables from the solar panels.



FIGURE 11 Electrical Boxes and Conduits to Pass Power to the SDAQ Using the Solar Panels.

After installing all the accelerometers and attaching them to the SDAQ system, the strain gauges were installed on the FRP sheets to monitor debonding of FRP sheets from the concrete surface. All strain gauges were covered and the wires from them were attached to the cables which transmit the signals from the strain gauges through the aforementioned conduit, to the SDAQ system located in the steel box. Environmentally protected strain gauges produced by Vishay, Inc. were used. The strain gauges were installed following standard installation techniques considering all cleaning and bonding requirements. Special epoxies were used to attach the strain gauges to the FRP sheets. Dead weights were put on top of the installed strain gauges to produce the required pressure to ensure the gauges were bonded. The strain gauges were left for 24 hours before connecting to the SDAQ. Fig. 12 shows the weights applied on top of each strain gauge to make sure they are attached completely to the FRP sheets. Fig. 13 shows one strain gauges after being covered by the rubber protection. Fig. 14 shows all strain gauges attached to the FRP sheets. Figure 15 shows concrete casting above the strain gauges.

Figure 16 showed the area strengthened with FRP after being batched with concrete and the sensor connections to the monitoring box.



FIGURE 12 Weights Applied on Top of Each Installed Strain Gauge.



FIGURE 13 Covered Strain Gauges Attached to the FRP Sheets.



FIGURE 14 All the Strain Gauges After Being Installed on the FRP Sheets and Connected to the Wires Transmitting the Strain Signals to the Data Acquisition (DAQ) Device.



FIGURE 15 Concrete Casting Over Area of Bridge Deck Strengthened with FRP



FIGURE 16 Top of Bridge Deck after Concrete Casting Showing the Connection of the Sensors to the Monitoring Box Under the Bridge

Moreover, four thermocouples were installed on the top surface and the underside of the bridge to measure the bridge temperature at both these points. Fig. 17 shows one of the thermocouple sensors attached to the web of the bridge girder.

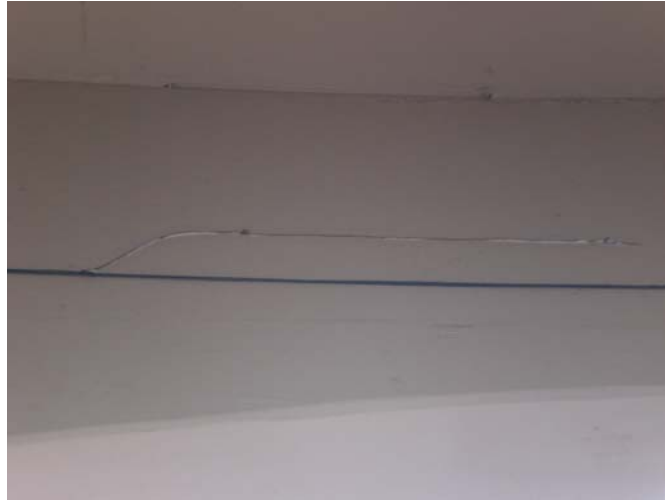


FIGURE 17 One Thermocouple Sensor Attached to the Web of the Bridge Girder.

Upon completion of the installation of all sensors on the bridge surface, they were connected through their cables to the SDAQ system housed in the steel box and located underneath the bridge. The SDAQ was connected wirelessly to the Worldwide Web. Fig. 18 shows the inside of the steel box with the SDAQ system and the wireless modem attached. The figure also shows the rechargeable battery for the solar cell, the digital timer and the power inverter that is required to switch the DC power obtained from solar panels through rechargeable batteries to the AC power that can be used by the SDAQ. The digital timer is programmed to schedule operation time. While the system can acquire data all the time, data transmission using wireless protocol has to be limited for wireless cost and for power limitations associated with using solar panels. As described in Report 2, the system is designed to operate for 8 hours daily.



FIGURE 18 Data Acquisition System, Rechargeable Batteries, Power Inverter, Digital Timer Switch and the Wireless Modem Located at the Steel Box.

The solar power was also successfully installed and is timed to work 8 hours every day. Special time for data download during low wireless activity is also scheduled. Fig. 19 and 20 show the solar power panels installed to provide clean renewable energy to the monitoring system and their connection to the monitoring system.

USER INTERFACE TO MONITOR BRIDGE 7937

With the SDAQ system and wireless modem, the user can monitor the bridge wirelessly through the World Wide Web. The DAQ system is programmed in such a way that gives the user an easy graphical interface to monitor the bridge and obtain data from all the sensors installed on the bridge. Moreover, the graphical interface gives the user the ability to control the SDAQ remotely by choosing the data and time frame to be saved on the DAQ device.



FIGURE 19 Solar Power System Installed on Bridge 7937 to Provide Clean Renewable Energy for The SHM System.



FIGURE 20 Solar Power System Installed on Bridge 7937 to Provide Clean Renewable Energy for The SHM System.

Moreover, the user can observe live data from each sensor at any time remotely. Fig. 21 shows the graphical interface that needs to be set up by the user to remotely observe the bridge data.



FIGURE 21 Graphical User Interface Shows the “Configuration” of Modules.

On the left side of Fig. 7, under the tab called “Configuration”, the user can change the rate of acquiring data from accelerometer and strain gauge modules from 2000 sample/ sec to 50,000 sample/sec. Moreover, the user has the ability to change the “Excitation Voltage” needed for strain gauge modules and the “Configuration” of strain gauges in Wheatstone bridge from “Half-Bridge” to “Full Bridge”. Two strain gauges are used on each spot of the FRP zone that compensates for temperature effect, producing what is known as a Half-Bridge strain gauges.

Fig. 22 shows the next tab of the above figure. This new view is called “File Setup” and shows how the files are time stamped based on the exact date, hour, minute and second they are acquired along with the base name of the file. File Setup can also give the user the ability to save the file automatically on the SDAQ for desired time duration and desired gaps between the files or save manually using a control switch.

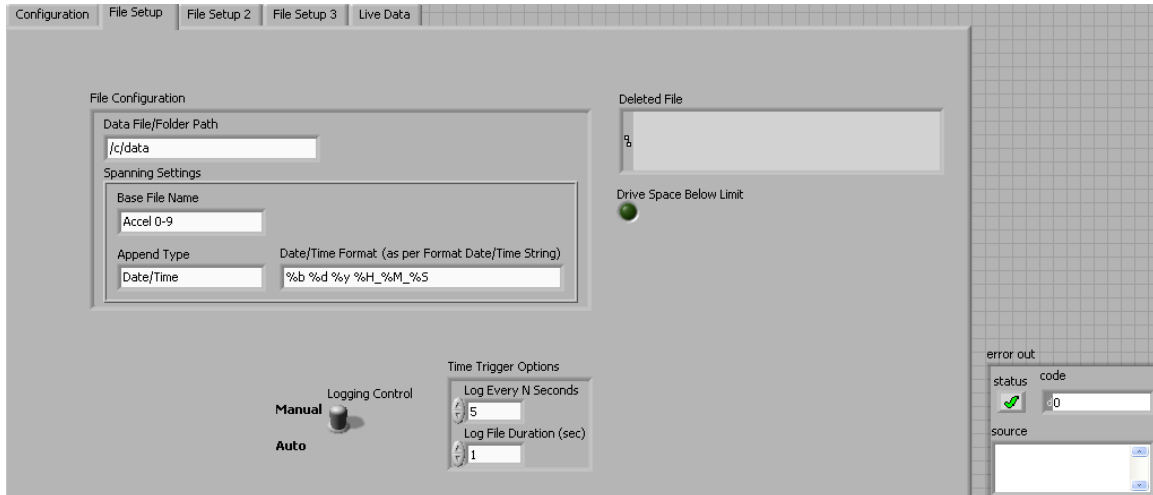


FIGURE 22 Graphical User Interface Shows “File Setup”.

As shown in Fig. 22, the base file name is Accel 0-9 which saves data from the first ten accelerometers. Saving data in three different categories (Accel 0-9, Accel 10-19, Strain) limits the size of each file to allow transfer of the file using FTP protocol wirelessly. It has been observed that one second duration of the saved file along with logging every five seconds are suitable numbers to acquire data from random traffic passing over the bridge. When the user puts the logging control on manual, no data is saved on the DAQ device until the logging switch which is located on the “Live Data” tab, as shown in Fig. 23, is turned on. When the logging switch turns on, the user can save data on the DAQ device for as long as the switch is on. Manually saving data is not recommended since different sizes of data will be saved on the SDAQ system that might be so large that sending it wirelessly won’t be feasible. “File Setup 2” and “File Setup 3” tabs shown in Fig. 23 are exactly the same as “File Setup” except they are designed for accelerometers 10-19 and strain gauges, respectively. The user can observe live data from each sensor.

Temperature data from all thermocouples can also be observed in Celsius Degree in the “Live Data” tab.

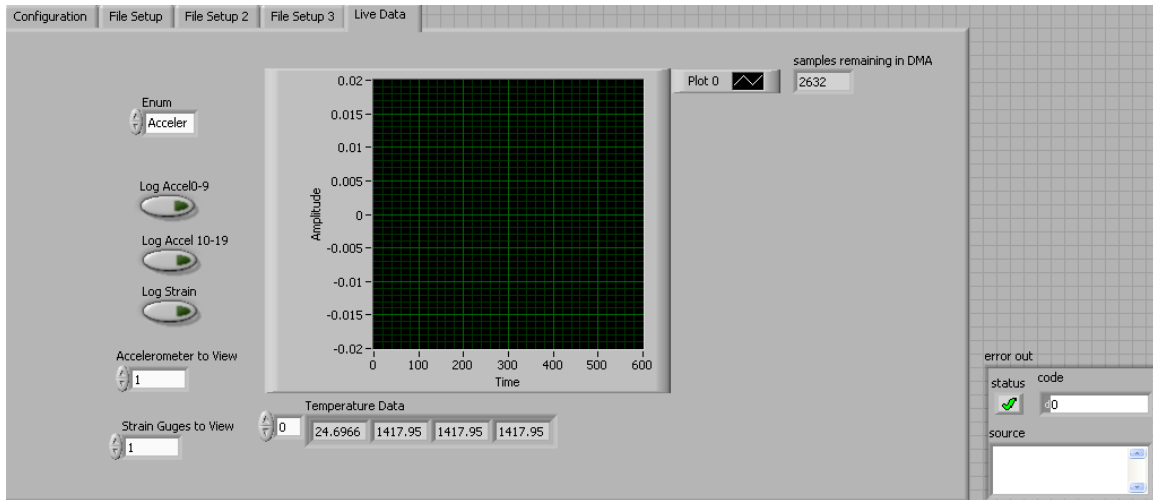


FIGURE 23 Graphical User Interface Shows “Live Data”.

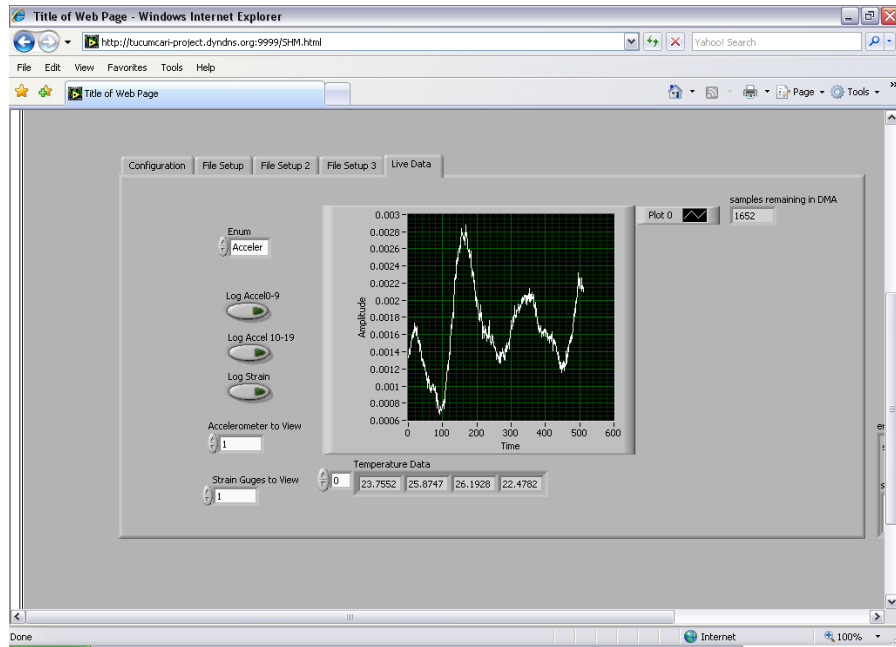
To use the graphical interface discussed above, the user needs to login to the web address given below in Internet Explore (IE).

[http:// tucumcari-project.dyndns.org:9999/](http://tucumcari-project.dyndns.org:9999/)

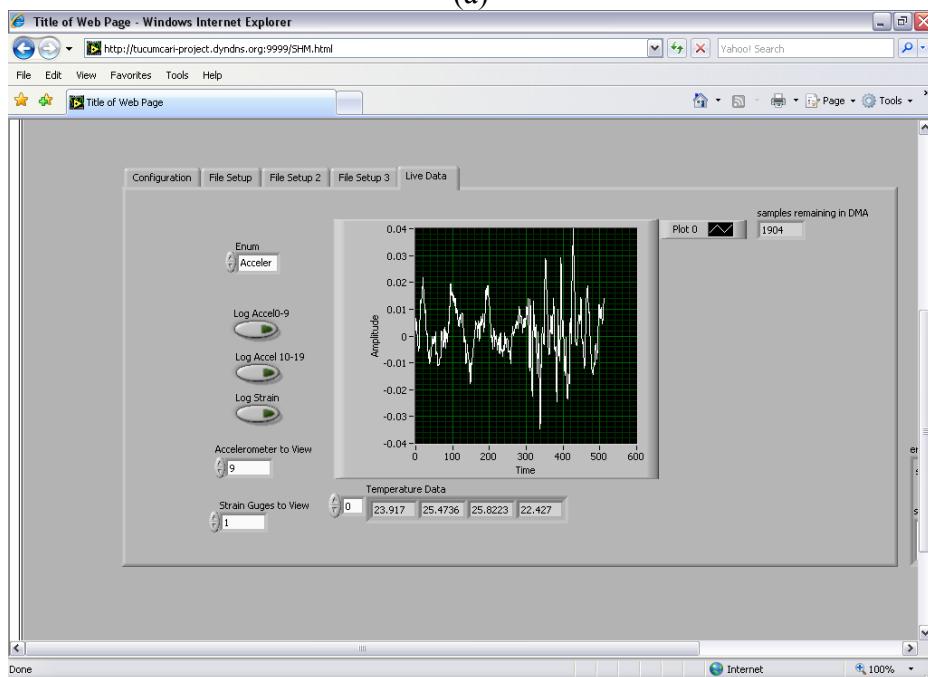
The website is specially made for the Tucumcari Bridge using dynamic DNS (dyndns.org) website. After using the web address given above, the user needs to put the following address in IE.

[http:// tucumcari-project.dyndns.org:9999/SHM.html](http://tucumcari-project.dyndns.org:9999/SHM.html)

Please note that the web address is case sensitive. A snapshot of this web address viewing live data from bridge 7937 is shown in Fig. 24.



(a)



(b)

FIGURE 24 Live Data From the Web Address to View Bridge 7937 recorded on June 26, 2009 (a) Acc 1 & (b) Acc 9.

If data recording is planned, it is important to know that the data will be stamped based on the sensors (accelerometers and strain gauges) and the exact time it was acquired. The

user then needs to use FTP protocol to transfer the data to a personal computer (PC). The web page the user needs in order to get the data is

<ftp://tucumcari-project.dyndns.org/>

The user should allocate a data folder and copy the data and paste it into the folder on the PC. Fig. 25 shows what will appear to the user after accessing the above address in IE.



FIGURE 25 FTP Graphical Interface for Transferring the Data from SDAQ.

DATA ANALYSIS FOR DAMAGE DETECTION

The files that are saved on the data acquisition device and transferred through FTP protocol have TDMS file format which is a format readable by special software for data acquisition. Special software is developed for reading and analyzing this data. The software called SMART-SHM is composed of two executable files that are designed to run on typical PC. The first file is called SMART-SHM-START.EXE which allows the user to view the data files downloaded from the bridge as “raw data” and to save them for further analysis. The second file called SMART-SHM-DAMAGE.EXE, is designed for

damage detection. On the first software SMART-SHM-START, the user has the ability to view all the sensors on the bridge and to display the synchronized data from the bridge for up to 4 sensors at the same time. Fig. 26 provides a snap shot of SMART-SHM-START software.

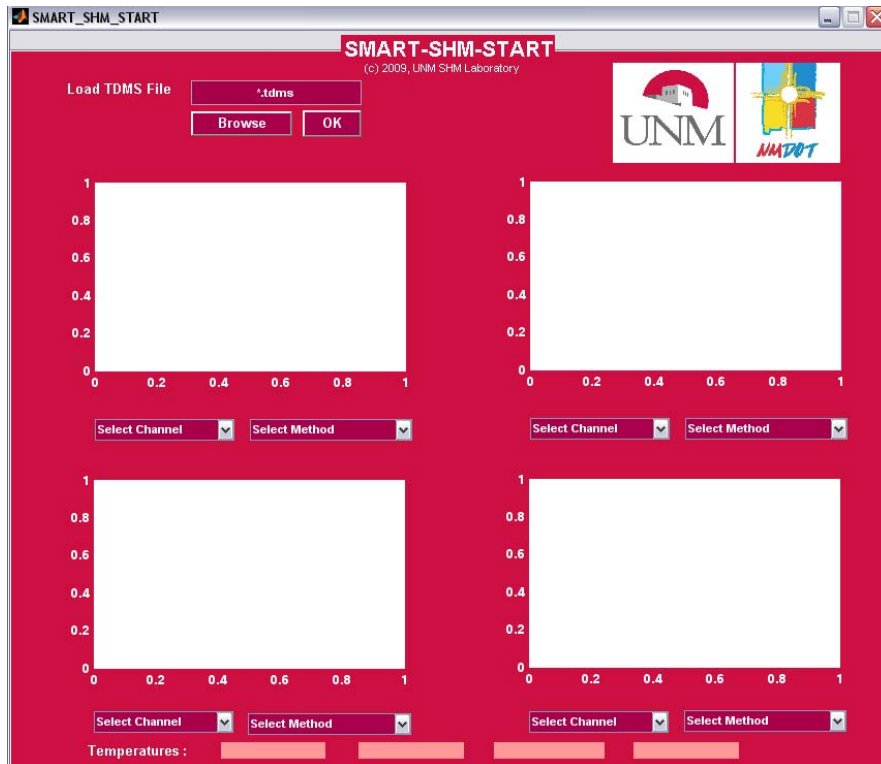


FIGURE 26 Snapshot of SMART-SHM-START Software Shows the Four Views That a User Can Display Synchronized Data in Them Along With the Temperature.

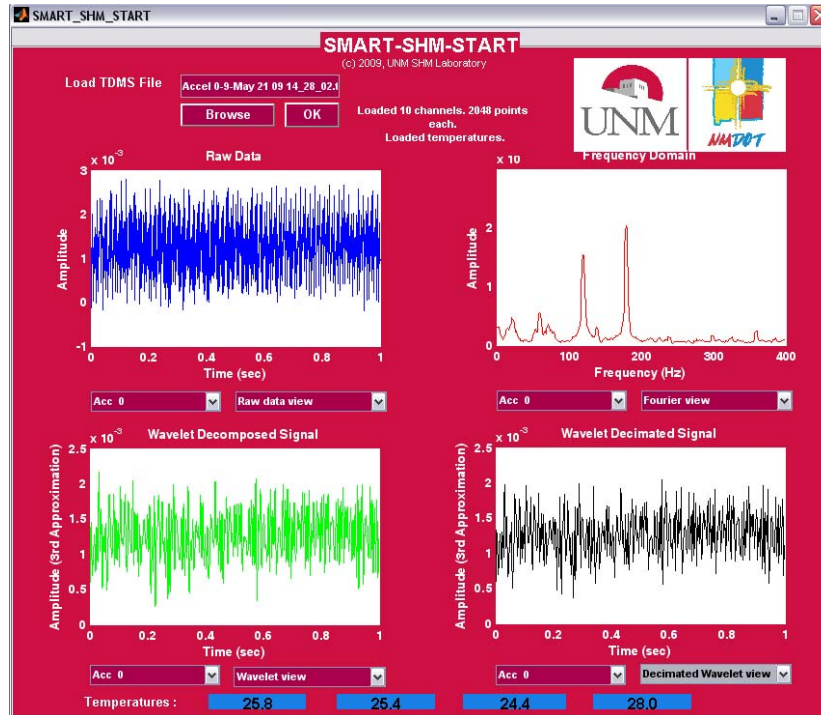


FIGURE 27 Raw Data Collected From Four Different Sensors With the Temperature Data as Shown in SMART-SHM-START Software.

The temperature data is shown at the bottom of the Software in degree Celsius. Fig.27 illustrates the raw data from four different sensors installed on the bridge along with the temperature data collected from four thermocouples on the bridge.

SMART-SHM-START also allows the user to perform basic analysis of the data. Four types of analysis are available. In addition to time domain data discussed above, fast Fourier transform and Wavelet transform can be performed and displayed. The software also allows the user to view a down-sampled wavelet transform of any desired sensor as shown in Fig. 28. In Fig. 28, it is shown that while the data was acquired from the bridge using 2 kHz sampling rate, the Wavelet transform smooths the signals and the high frequency components of signals are eliminated from the original signal. The down-sampled Wavelet transform will have a sampling frequency of 400 Hz.

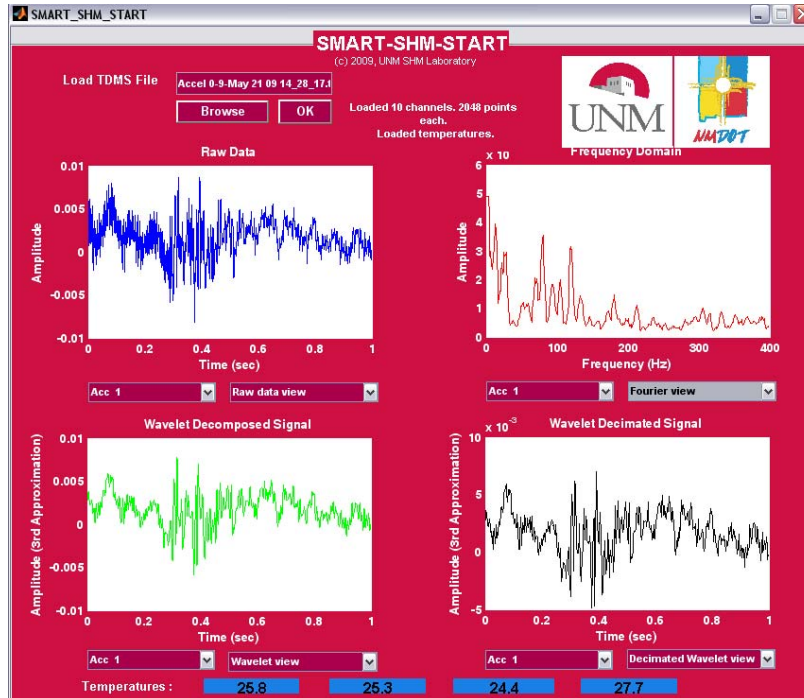


FIGURE 28 SMART-SHM-START software shows raw data, Fourier transform, Wavelet transform and decimated Wavelet signals collected from sensor 8 installed on the bridge. The bottom row shows the temperature at four locations on the bridge.

To detect damage on the bridge, software was coded and produced. The second software, called “SHM-SMART-DAMAGE”, was designed to perform damage feature extraction using wavelets and fast Fourier transform and to display the history of the bridge damage feature. Fig. 29 illustrates the SHM-SMART-DAMAGE software for damage detection of the bridge.

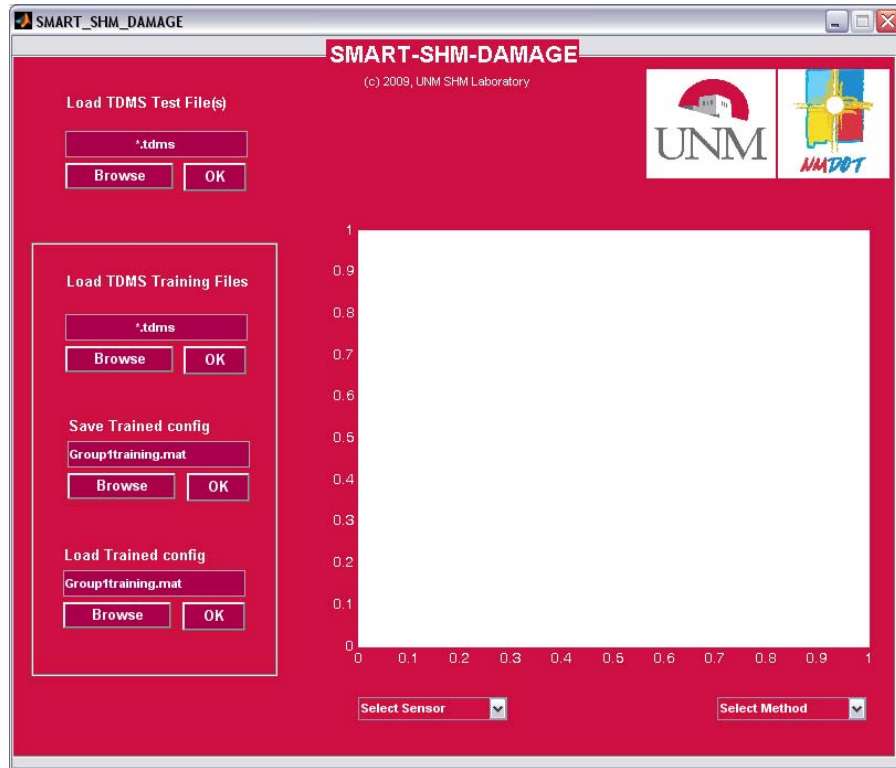


FIGURE 29 Snap Shot of SHM-SMART-DAMAGE Software Designed for Observing Bridge Behavior and its Change Over Time.

The first thing required to operate the SHM-SMART-DAMAGE is to load the TDMS Training files, to train the software based on available data gathered during a period of time from the bridge. Since the data gathered wirelessly and randomly from the bridge is a large data set, it is needed for the training process. The training data set is used to establish the boundaries of the damage feature (being Wavelet or Fourier). The boundaries were established at 99.7% probability. After the training data is loaded, a new dataset can be loaded. Here, two different methods are used for detecting damage on the bridge:

First, Fast Fourier Transform, which transforms the raw data from the bridge in the time domain to the frequency domain, is used. When damage occurs to the bridge, the main frequency components of the bridge might change and therefore the maximum frequency

of acceleration signals will change. Since the bridge has very large stiffness and mass, the small damages shouldn't be able to change the major frequency components of the bridge. The maximum signal frequency was limited to 45 Hz since the signals with higher frequencies usually represent noise. In the training part of this method, the maximum frequency of signals at each sensor is computed for each training data set and the mean value of all data sets is used for the training process. The upper and lower limits for the healthy state of the bridge are calculated based on 99.7% probabilities not to exceed the mean. This is represented graphically in the software. For any new data set, the software will display its location on the chart with respect to the mean boundaries. It should be noted that lack of enough training of the data sets may give false alarms using this method.

Second, the energy of signals calculated in the wavelet domain is used as a damage feature to differentiate between healthy and damage states of the bridge. The acceleration signal is decomposed into approximation and detail signals with low and high frequency components, respectively using Wavelet transform. Using Wavelet decomposition tool, the acceleration signals are decomposed into a group of signals with different frequencies.

The decomposed signal of $x'(n)$ at level p can be computed as

$$x'(n) = \sum_{k=-\infty}^{\infty} a_{p,k} \cdot \phi_{p,k}(n) + \sum_{j=1}^p \sum_{k=-\infty}^{\infty} d_{p,k} \cdot \varphi_{p,k}(n) \quad (1)$$

where $x'(n)$ is the decomposed signal. Moreover, $\phi_{p,k}(n)$ and $\varphi_{p,k}(n)$ are the scaling and wavelet basic functions, respectively. In this SHM system for bridge 7937, the scaling and wavelet functions are selected for the *Daubechies db4* mother wavelet. The approximation coefficients $a_{p,k}$ and the detail coefficients $d_{p,k}$ are calculated as

$$a_{p,k} = 2^{(-p/2)} \sum_n x(n) \phi(2^{-p}n - k) \quad (2)$$

$$d_{p,k} = \sum_n x(n) \varphi_{p,k}(n) \quad (3)$$

The signals were down-sampled from 2 KHz to 400 Hz sampling rate. Then the third resized approximation A_{3R} of the acceleration signal is used to compute the damage feature as shown in Eq. 4.

$$\lambda = \sum_k (a_{3,k})^2 \quad (4)$$

The damage feature (metric) λ represents the energy of the third approximation signal computed over a time window. Experimental and analytical investigations (3, 4, 5 and 2) have proven the ability of the proposed damage metric λ to detect and quantify damage occurrence on bridge structures.

Using the energy of the wavelet decomposed signals, the training data sets were computed. The mean value and 99.7% boundaries were established. For any new data set obtained from the bridge, if the energy of signals calculated in the wavelet domain at the location of each sensor passes the established boundaries, the bridge might be experiencing damage near the location of that sensor. It should be noted again that to not get false alarms about damage on the bridge, the training process should be done for large numbers of data sets gathered from the bridge at different times. It is also worth mentioning that the damage features, discussed above, are calculated at the location of each sensor and in this case each sensor has independent damage value from the other sensors. Fig. 30 represents a snapshot of the SMART-SHM-Damage software showing the mean and boundaries of the Fourier transform damage feature at sensor 1. It can be observed in the snapshot that 10 datasets were used to establish the damage boundaries.

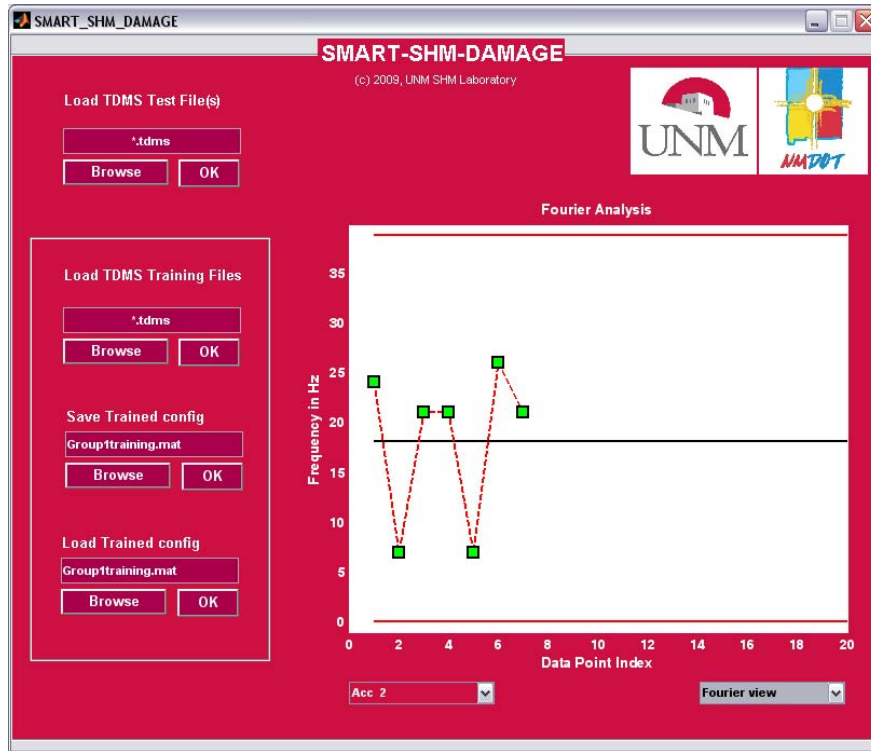


FIGURE 30 Snapshot of SMART-SHM-Damage Shows the History of the Frequency Damage Feature at Sensor 1 as Extracted From Bridge 7937.

As it is obvious from Fig. 30, the frequency mean value of all training data sets is around 20 Hz while the lower and upper limits will be between -5 and 40 Hz. Moreover, it is apparent that all the frequencies are within the established range that confirms the healthy state of the bridge. Fig. 31 represents a snapshot of the SMART-SHM-Damage software showing the mean and boundaries of the wavelet transform damage feature at sensor 8.

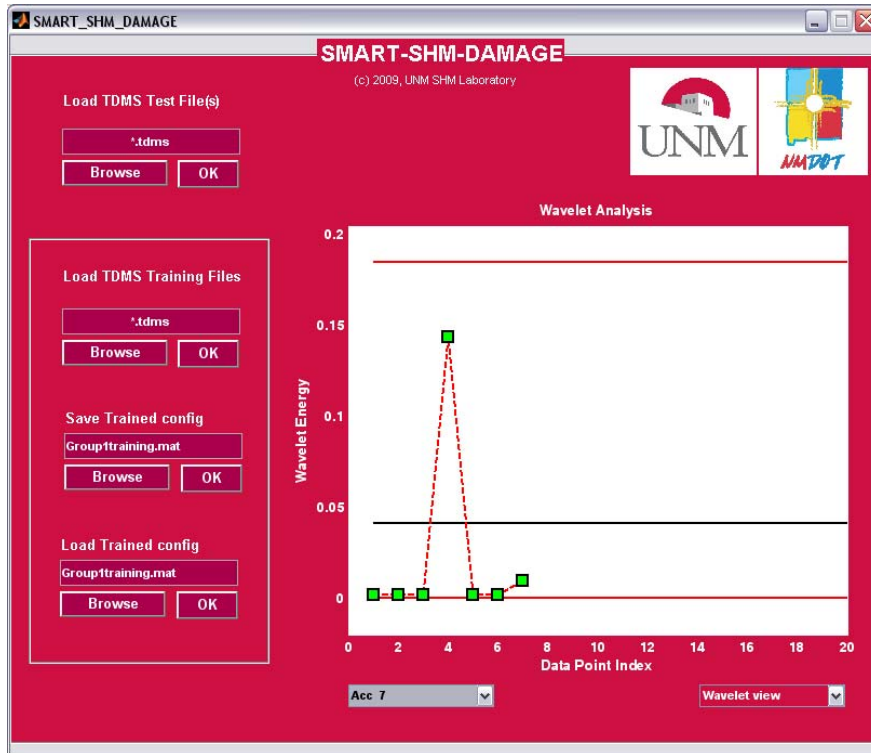


FIGURE 31 Snapshot of SMART-SHM-Damage Show the History of the Wavelet Damage Feature at Sensor 8 as Extracted From Bridge 7937.

As shown in Fig. 26, the mean value of energy of signals calculated in the Wavelet domain at sensor 8 is around 0.05 while the lower and upper limits calculated from the mean value plus or minus three times of the standard deviation calculated at the location of sensor 8 are -0.1 and 0.2, respectively. It can also be concluded that for 9 different data sets obtained at different times, no damage has occurred near sensor 8 since all the results are located within the established healthy limits.

It should also be mentioned that the SMART-SHM-DAMAGE software made for this project has the ability to show up to 20 different data sets obtained from the bridge at different times in order to give the user a sense of the history of the. Finally, the user is capable of saving the configuration of all the files obtained from the bridge to compare to

new data sets at a later date. Moreover, the user can also save the configuration of the files used for training of the program and use different data sets as training files.

CONCLUSION

This report described the installation and operation of this new SHM system for monitoring bridge 7937 in Tucumcari, New Mexico. The new system is powered with clean renewable solar energy. Software to observe and communicate the data over the bridge is described. Software for data analysis and damage detection is also described and their use is explained. The new system is currently operational and shall enable a case study for smart monitoring of structures for public safety.

REFERENCES

1. AASHTO. *LRFD Bridge Design Specifications, Manual for Condition Evaluation of Bridges*. Interim revisions, Second Edition. American Association of State Highway and Transportation Officials, Washington, D.C., 2006.
2. Azarbayejani, M., A. El-Osery, K.-K. Choi and M.M. Reda Taha. Probabilistic Approach for Optimal Sensor Allocation in Structural Health Monitoring. *Smart Materials and Structures*, Vol. 17, No. 5, 2008, paper # 055019.
3. Reda Taha, M., A. Noureldin, A. Osman and N. El-Sheimy. Introduction to the Use of Wavelet Multi-Resolution Analysis for Intelligent Structural Health Monitoring. *Canadian Journal of Civil Engineering*, Volume 31, Issue 5, 2004, pp. 719-731.
4. Horton, S., M.M. Reda Taha and T. J. Baca. A Neural-Wavelet Damage Detection Module for Structural Health Monitoring, In *Proceedings of International Workshop on Structural Health Monitoring*, Chang, Fu-Kuo, Ed., Stanford, USA, 2005, pp. 556-564.
5. McCuskey, M., M.M. Reda Taha, S. Horton and T. J. Baca. Identifying Damage in ASCE Benchmark Structure using a Neural-Wavelet Module. In *Proceedings of the International Workshop on Structural Health Monitoring*, Granada, Spain, July 2006, pp. 421-428.



New Mexico Department of Transportation
RESEARCH BUREAU
7500B Pan American Freeway NE
PO Box 94690
Albuquerque, NM 87199-4690
Tel: (505) 841-9145